

Use Authorization

In presenting this thesis in partial fulfillment of the requirements for an advanced degree at Idaho State University, I agree that the Library shall make it freely available for inspection. I further state that permission to download and/or print my thesis for scholarly purposes may be granted by the Dean of the Graduate School, Dean of my academic division, or by the University Librarian. It is understood that any copying or publication of this thesis for financial gain shall not be allowed without my written permission.

Signature _____

Date _____

A STUDY OF THE POTENTIAL PERFORMANCE AND FEASIBILITY OF A
HYBRID-FUEL OPEN CYCLE GAS CORE NUCLEAR THERMAL ROCKET

by

Lucas Beveridge

Thesis

submitted in partial fulfillment

of the requirements for the degree of

Master of Science in the Department of Nuclear Engineering and Health Physics

Idaho State University

Summer 2016

To the Graduate Faculty:

The members of the committee appointed to examine the thesis of LUCAS BEVERIDGE find it satisfactory and recommend that it be accepted.

Jay Kunze,
Major Advisor

Richard Schultz,
Committee Member

Brian Williams,
Graduate Faculty Representative

VITA

Lucas was born and raised in Oregon. From a very young age, he was inspired to be an engineer, and pursued electronics and model rockets. In high school, he led a group of fellow students in the Team America Rocketry Challenge, which went to the national finals in 2003. He then attended Embry Riddle Aeronautical University to pursue Aerospace Engineering and Space Physics, and graduated in 2010 with a B.S. in Space Physics. Lucas is currently a graduate student at Idaho State University studying Nuclear Science and Engineering, and will soon begin working on his PhD.

TABLE OF CONTENTS

LIST OF ILLUSTRATIONS	vii
LIST OF FIGURES	viii
LIST OF TABLES	ix
LIST OF ABBREVIATIONS.....	x
GLOSSARY	xi
Abstract	xii
Chapter I: Introduction.....	1
Motivation for Nuclear Propulsion	1
Research Questions	3
Assumptions and Limitations	8
Relevance	9
Chapter II: Literature Review	10
Introduction to the Literature on Nuclear Thermal Propulsion	10
Conclusions.....	11
Chapter III: Methodology	13
Research Approach	13
MCNP6 and Basic Reactor Physics	14
Refined MCNP Models.....	16
Solid-Core Heat Transfer	26

Reactor Cavity Heat Transfer	29
Chemical Equilibrium and Specific Impulse	30
Mission Analysis.....	32
Chapter IV: Results.....	34
Power Ratio Determination and Cooling Requirements.....	34
Critical Mass Comparison.....	35
Reactivity Effects.....	36
Fuel Leakage.....	41
Specific Impulse and Mission Architecture	46
Chapter V: Conclusions	54
Discussion of Research Findings	54
Future Research Possibilities	55
References.....	57

LIST OF ILLUSTRATIONS

Illustration 1. Basic Open Cycle Gas Core Rocket (OCGCR)	3
Illustration 2. Mini-Gas Core Concept.....	5
Illustration 3. Hybrid Reactor Core Concept	7
Illustration 4. Basic MCNP model.....	15
Illustration 5. Refined hybrid engine	18
Illustration 6. All three engines.....	24
Illustration 7. NASA NTR MTV	33
Illustration 8. Fuel Displacement Due to Acceleration.....	39
Illustration 9. Conjunction and Opposition Class Mission Trajectories	49
Illustration 10. Conjunction Class Δv vs Launch Window.....	50
Illustration 11. In-Situ MTV Propellant Production	53

LIST OF FIGURES

Figure 1. Fuel Radius vs Reactivity Worth (note the difference in slopes).....	37
Figure 2. Reactivity Worth of Various Perturbations.....	40
Figure 3. Low- ϵ Engine Relative Leakage due to Kelvin-Helmholtz Instability vs Flow Velocity.....	44
Figure 4. High- ϵ Engine Relative Leakage due to Kelvin-Helmholtz Instability vs Flow Velocity.....	45

LIST OF TABLES

Table 1. MCNP model details, pure gas core 19

Table 2. MCNP model details, low ϵ_{gas} core..... 20

Table 3. MCNP model details, high ϵ_{gas} core 21

Table 4. Comparison of Energy Deposition Reactivity Change for two Gas Fuels 25

Table 5. Fuel composition of each core 25

Table 6. High- ϵ Engine Energy Deposition 34

Table 7. Low- ϵ Engine Energy Deposition..... 34

Table 8. Critical Masses..... 36

Table 9. Maximum Allowable Density Change Corresponding to \$1 worth 38

Table 10. Relative Leakage, r for all Scenarios..... 46

Table 11. Low- ϵ Engine Performance Results..... 47

Table 12. High- ϵ Engine Performance Results..... 47

Table 13. Pure-Gas Engine Performance Results 48

Table 14. Inert Mass Fractions for Mars Mission Orbital Maneuvers..... 51

Table 15. Spacecraft Masses and Initial Propellant Load (all units in metric tons) 51

LIST OF ABBREVIATIONS

OCGCR	Open-Cycle Gas Core Reactor (or Rocket)
NTR	Nuclear Thermal Rocket
MCNP	Monte Carlo, N-Particle, a particle transport code developed by Los Alamos National Lab
CEA	Chemical Equilibrium Applications, a chemical equilibrium code developed by NASA
NERVA	Nuclear Engine for Rocket Vehicle Applications
AEC	Atomic Energy Commission (US federal agency, replaced in 1978 by the Department of Energy and the Nuclear Regulatory Commission)
ENDF	Evaluated Nuclear Data File (contains nuclear cross section data for numerous isotopes and materials, maintained by Brookhaven National Lab)
MTV	Mars Transfer Vehicle
CFD	Computational Fluid Dynamics, a class of computer codes that simulate the behavior of fluids
TMI	Trans-Mars Injection (maneuver)
MOI	Mars Orbit Insertion (maneuver)
TEI	Trans-Earth Injection (maneuver)
MAV	Mars Ascent Vehicle
ISRU	In-Situ Resource Utilization

GLOSSARY

Specific Impulse, I_{sp}	The amount of impulse delivered to a vehicle per unit of propellant consumed. It can be expressed as the ratio of engine thrust to weight-flow rate of propellant. Typically has units of seconds.
Δv	Velocity change increment.
NERVA	A NASA/AEC program that ran from the late 1950's until the early 1970's to develop a nuclear powered rocket engine. The reactors all had solid fuel (namely UO_2 in graphite). Numerous reactors and engines were tested at the Nevada Test Station at Jackass Flats. The program eventually produced an engine that could have been flown.
Nuclear-Electric Propulsion	Any electric propulsion system (i.e. electrostatic thrusters, Hall thrusters, plasma thrusters, etc.) powered by a reactor with an electric conversion system.
Conjunction-Class mission	A minimum energy, long duration mission scenario
Opposition-Class mission	A mission scenario with shorter transit times, and with shorter stays on Mars
Hohmann transfer	An orbit change maneuver with two short impulses that requires the least amount of energy to get from one circular orbit to another
ϵ_{gas}	Ratio of power produced in the gas core region to the total reactor power, $\epsilon_{gas} = p_{gas}/p_{total}$
ϵ_{solid}	Ratio of power produced in the solid core region to the total reactor power, $\epsilon_{solid} = p_{solid}/p_{total}$
High- ϵ engine	The hybrid reactor examined in this study with a higher ϵ_{gas} of ~ 0.673 (see definition above)
Low- ϵ engine	The hybrid reactor examined in this study with a lower ϵ_{gas} of ~ 0.51 (see definition above)

A STUDY OF THE POTENTIAL PERFORMANCE AND FEASIBILITY OF A
HYBRID-FUEL OPEN CYCLE GAS CORE NUCLEAR THERMAL ROCKET

Idaho State University (2016)

Abstract

The goal of this thesis work was to investigate a type of nuclear thermal rocket that has many of the advantages of open-cycle gas core rockets, while alleviating some of the drawbacks. Chemical rockets are limited in specific impulse due to the high molecular weight of the exhaust products, and the operating temperature. Solid-core nuclear thermal rockets can have much lower molecular weight exhaust (using hydrogen as propellant), but have operating temperatures no higher than $\sim 3000\text{K}$ due to the material limitations of the fuel. One possible solution is to use a gaseous fuel that can run at indefinitely high temperatures, but controlling the reactivity and containing the fuel has historically proven to be challenging. The current work focuses on a hybrid-fuel reactor with solid and gaseous fuel. The reactor cavity is surrounded by solid fuel which provides upwards of 50% of reactor power. This reduces the amount of gaseous fuel, which resulted in smaller reactivity fluctuations, and reduced fuel leakage while maintaining a high performance (with specific impulses still around 1600 to 2000 Sec.). Reactor designs were evaluated with MCNP6, and the specific impulse (and exhaust composition) was determined with NASA's CEA code. Hypothetical scenarios for conjunction-class Mars missions were compared to similar missions using chemical and conventional NTR propulsion.

Chapter I: Introduction

Motivation for Nuclear Propulsion

For any spacecraft to change orbits or maneuver, it needs some associated velocity change. From Newton's third law, this Δv can be related to the change in vehicle mass and the specific impulse (or exhaust velocity) of the engine [1]:

$\Delta v = I_{sp} g_0 \ln \left(\frac{m_0}{m_1} \right)$. Where g_0 is sea level gravitational acceleration, m_1 is the burnout mass of the vehicle (dry mass), and m_0 is the initial mass of the vehicle (wet mass). The specific impulse (I_{sp}) is the change in vehicle momentum per unit of propellant consumed, and is therefore a measure of the rocket engine performance. It's usually defined as the thrust per weight flow rate of propellant (and thus has units of seconds, so that either imperial or metric unit systems will produce the same value). It can also be thought of as the length of time a unit weight of propellant will produce a unit force of thrust (assuming the same units as weight).

Specific impulse can also be related to the exhaust velocity: $I_{sp} = \frac{v_e}{g_0}$. However, the exhaust velocity is a function of the fluid properties of the exhaust. The exhaust velocity of an ideal rocket in a vacuum is [1]:

$$v_e = \sqrt{\frac{2 R T \gamma}{(\gamma - 1) M}} \quad (1)$$

Here, T is the exhaust temperature of the propellant, R is the universal gas constant, γ is the ratio of specific heats, and M is the molecular weight of the exhaust products. Clearly, increasing the temperature and/or decreasing the molecular weight of the exhaust products will increase the exhaust velocity, and thus also the specific impulse. Also, at high enough temperatures, the propellant molecules can dissociate, and

reduce the molecular weight of the exhaust products which further increases the exhaust velocity. This is especially true of Hydrogen, which (if dissociated into free-atoms) has the lowest possible molecular weight of any propellant (not including exotic particles, such as would be produced in an anti-matter rocket). However, Hydrogen only begins to significantly dissociate at extremely high temperatures (>5000 K), which are far beyond the material limitations of a solid-fuel core such as a NERVA reactor. Chemical propellants are limited in both temperature and molecular weight, due simply to the limited enthalpy and heavy molecular weight products of combustion (or in some cases exothermic decomposition). The highest performance chemical propellants are Hydrogen and Oxygen, which when burned produces mostly water as the exhaust product, which is several times heavier than Hydrogen alone.

Nuclear thermal rockets operate by adding enthalpy to the propellant in the reactor core, but the propellant can only reach temperatures of around 3000K before the fuel/fuel-matrix starts melting. The obvious solution here is to use gaseous or liquid fuel. Indeed, there have been numerous gas and liquid fuel nuclear rocket concepts proposed, but the concept with the highest performance, and perhaps most well studied is the open cycle gas core rocket (OCGCR). In it, the propellant flows around the dense gas fuel within a cavity, where they come into direct contact. The fuel is held in the cavity by hydrodynamic forces [2] (see Illustration 1).

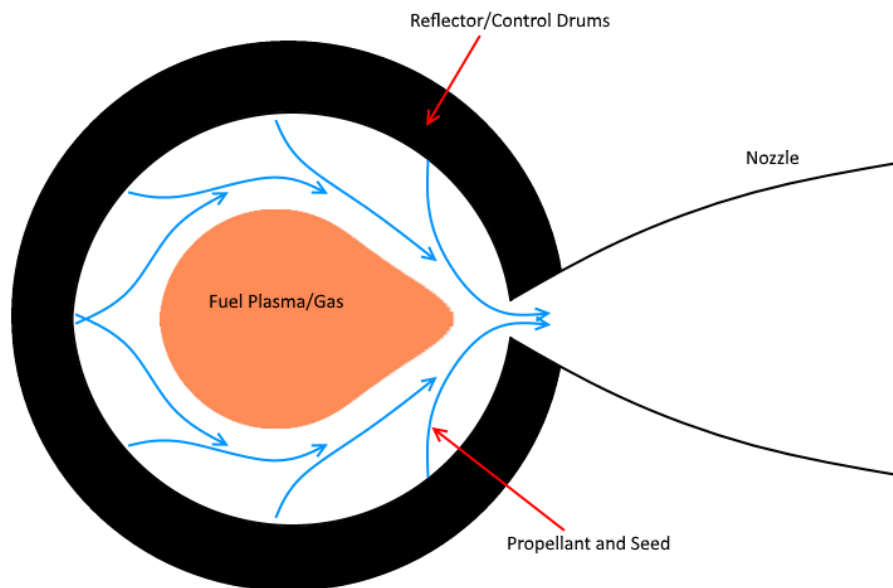


Illustration 1. Basic Open Cycle Gas Core Rocket (OCGCR)

Heat transfer to the propellant is primarily through radiation. The fuel is therefore much hotter than the propellant, but this isn't an issue because it is not near the cavity wall, and most of the energy is absorbed in the propellant. A seed material (such as graphite particles) must be added to the propellant to absorb more of the radiation since the propellant is mostly transparent to infrared and visible light [3].

Research Questions

There are a number of issues with the open-cycle gas core rocket (OCGCR). First, because there is no physical barrier between the fuel and propellant, some of the fuel will inevitably leak out. This decreases performance by increasing the exhaust molecular weight, and increases mission cost because replacement enriched Uranium needs to be carried safely onboard the vehicle. Second, controlling the reactor can be difficult due to reactivity changes caused by the fuel moving or changing shape within the core. Third,

the core is usually quite large and heavy compared to a chemical or solid-core engine. This is because in order to obtain a reasonable critical mass, the fuel density must be quite high to achieve critical mass within a reasonable volume, which also means that the core pressure (at high temperature) must also be very high [2] resulting in a very heavy pressure vessel.

To alleviate some of these problems, one concept called the ‘Mini-Gas Core’, developed by Robert Hyland has the cavity surrounded by a solid fuel “driver-core” which contributes most of the overall reactivity [4]. This dramatically reduces the amount of gas-fuel, and makes the engine much smaller and lighter. This concept was originally developed by Hyland to alleviate specific problems that were encountered during criticality tests of a gas core reactor, such as allowing uranium metal wire to be fed into the cavity without vaporizing it before reaching the fuel. However, because the driver-core is generating most of the reactor’s power (about 80%), it requires greater cooling than just the cavity wall. The obvious solution might be to simply cool it with the cold propellant before injecting it into the gas-core. However, because the gas-core region would only generate ~20% of the reactor’s power, it would not heat the propellant significantly more than the solid core. Therefore the performance would not be competitive with a solid-core NERVA type engine. Therefore, the driver-core would have to be cooled externally with radiators that are quite heavy, and so the overall engine power would be severely limited to minimize engine mass. The result is an engine that produces slightly more thrust, and with comparable mass (10 mt) to large nuclear-electric systems, but with a much lower specific-impulse (2000 S. vs. 6000 S.) [1], [5]. Therefore, if the fraction of the reactor power produced in the gas fuel can be increased, then the

solid-fuel can be cooled by the propellant, while maintaining a high specific-impulse and high power. This power ratio, denoted by ϵ_{gas} (power produced in gas core/total reactor power) is an important parameter, and is used extensively in the current work. An illustration of the Mini-Gas Core concept is shown in Illustration 2.

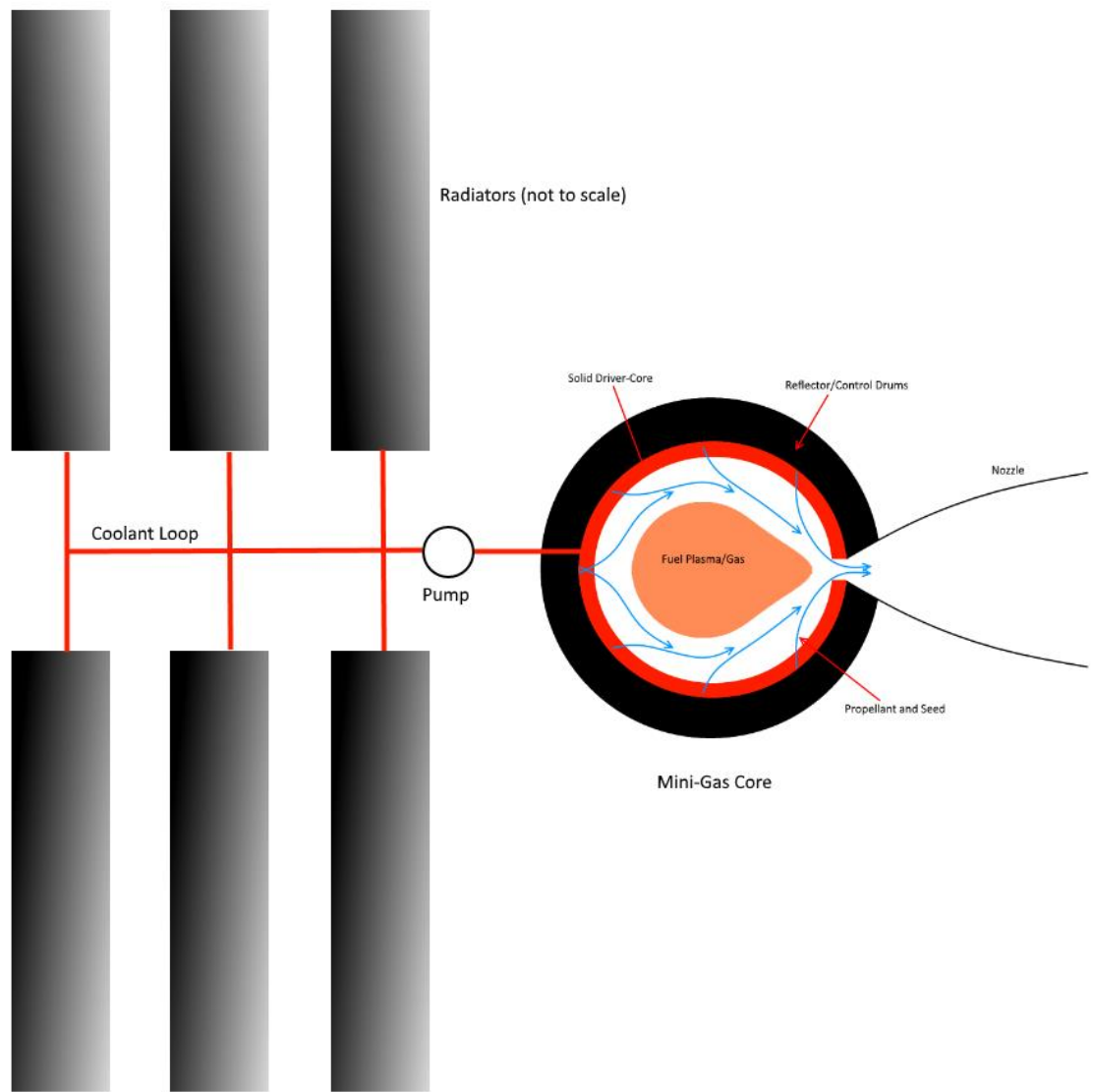


Illustration 2. Mini-Gas Core Concept

In this study, the goal was to develop an engine concept with some of the benefits of both the OCGCR and the Mini-Gas Core. This was done by evaluating various reactor designs until several were found with $\epsilon_{\text{gas}} \geq 50\%$. This is important for eliminating the

radiators that cool the solid core. For example, if we assume that the solid core produces 80% of the power, and that the solid core operating temperature can't go above 3000K, then the gas core will only heat the propellant another ~500K for total exhaust temperature of 3500K, which does not substantially increase the exhaust velocity beyond that achievable with an ordinary solid-core NTR. However, if $\epsilon_{\text{gas}} = 0.5$, then the gas core will add an additional ~2400K for a total exhaust temperature of 5400K. In addition to the performance increase from the higher temperature, it's also hot enough to dissociate much of the molecular hydrogen propellant into atomic hydrogen, which could potentially increase the exhaust velocity by as much as a factor of $\sqrt{2}$.

To make the difference more explicit, let's use the temperatures above, and the equation for exhaust velocity already defined to compare them. The specific heat ratio can be looked up in a table see [1] (pg. 93 and 94). However, estimating M for the high temperature case is more complicated because it's difficult to estimate how much of the Hydrogen has dissociated. For this example, we'll just assume all the Hydrogen is atomic (M=1) for the 5400K case, and M=1.5 for the 3500K case, and so $\gamma(3500\text{K})=1.27$, and $\gamma(5400\text{K})=1.25$. The result for the 3500K case is $v_e=13,341$ m/s which is equivalent to a specific impulse of about ~1300 Sec. However, for the 5400K case, the $v_e=21,148$ m/s, or a specific impulse of about 2100 Sec. The difference is even greater for $\epsilon_{\text{gas}} = 0.75$, but because there is more gas fuel, the reactor may be more difficult to control, and more fuel may leak out during operation, which eliminates some of the advantages over a gas core.

Because the radiators are no longer needed to cool the solid core, the maximum power is not limited. Indeed, the assumed maximum operating power for all the reactors studied was 3GWth. According to the most recent NASA Design Reference Architecture

for a human Mars mission, a typical inert mass for the Mars Transfer Vehicle (MTV) that carries the crew from Earth orbit to Mars orbit and back, is about 30mt [6], resulting in a worst case acceleration of about 1g (for a single engine). A basic illustration of the engine concept is shown in Illustration 3.

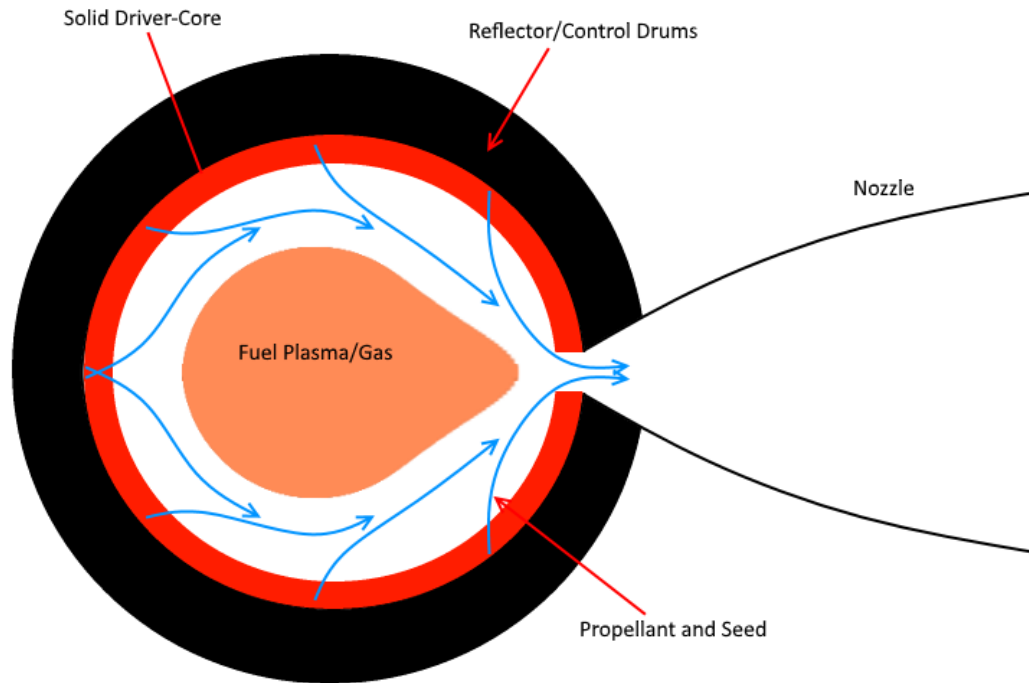


Illustration 3. Hybrid Reactor Core Concept

To determine if the hybrid concept offers any real advantages over the pure gas core concept, the changes in reactivity from various types of perturbations, actual engine temperatures and performance, and fuel leakage rates needed to be compared. This is discussed in greater detail in the next section.

Another potential issue investigated was that of heat transfer in the solid core. Because there is less fuel and supporting fuel matrix, all of the convective heat transfer to

the propellant must take place in a very small volume. To address this, graphite foam was examined as a matrix material due its high specific surface area (5,000 to 50,000 m²/m³), high thermal conductivity, and high temperature tolerance [7]. Thankfully, graphite foam is already being used in heat exchangers and other applications, so there is ample literature on how to estimate Nusselt number, heat transfer coefficients, and pressure loss based on the porosity and structure of the foam [8].

Assumptions and Limitations

Many different hybrid (solid and gas fuel) concepts were investigated in this study with MCNP-6, a Monte-Carlo particle transport code developed at Los Alamos National Lab. MCNP is able to determine how much energy is deposited (from all possible sources) into different reactor regions. This then allows a determination of ϵ_{gas} . After some trial and error, several different hybrid reactors were found that had $\epsilon_{\text{gas}} > 50\%$ (for a critical mass). Two of these were chosen for further investigation into reactivity and fuel leakage. An OCGCR reference core was also studied that was identical to the hybrid cores, but with all gaseous fuel. Therefore, there could be a direct comparison between two hybrid cores (one with $\epsilon_{\text{gas}} = 50\%$, and the other $\epsilon_{\text{gas}} = 67\%$), and a pure gas core.

Comparisons were made of the critical mass of the three cores. The power for all three was assumed to be 3GW. This much power would provide a great deal of thrust, even at high specific-impulse. The low- ϵ core (50%) had the lowest critical mass, the high- ϵ core (67%) was larger, and the pure-gas core was larger still. This agrees with the NASA mini-gas core rocket results, albeit it much larger reactors.

Using MCNP-6, the reactivity change caused by several different possible perturbations were studied. The possible effects investigated were that of the 1) gas fuel

expanding and contracting due to density changes, 2) displacement of the fuel within the core (as would be caused by the vehicle accelerating), 3) loss of propellant, 4) the addition of seed material in the propellant (to absorb the radiative heat from the fuel), and the addition of fuel to the propellant due to leakage. Seed material is needed because the propellant is mostly transparent to the radiation emitted by the fuel in the cavity, so for adequate heat transfer, the propellant must absorb most of this radiation. For all cases, the reactivity change ($\% \Delta k/k$) for the hybrid cores was lower than the pure gas OCGCR, as expected.

Relevance

Several times over the past 40 years, NASA has been given mandates to develop plans for sending crews to Mars. Most of these were in the last 25 years. In addition, private companies have begun to reduce the cost of launching, and some also intend to send people to Mars. All of this bodes well for deep space exploration in the coming years, and will make high performance propulsion systems more appealing. If any of these companies succeed at making planetary exploration profitable, then advanced propulsion will likely eventually take the place of chemical propellants to make in-space vehicles more economical. In the most recent published outline for crewed Mars missions, NASA even examined NTR's as one of the propulsion options for the Mars transfer vehicle [6] (this vehicle takes the crew from Earth orbit to Mars orbit and back to Earth). In this sort of environment, if a gas-core rocket were to appear more feasible, it may get developed further.

Introduction to the Literature on Nuclear Thermal Propulsion

Nuclear power has long been known to have the potential to increase the performance of space propulsion systems, and during the 1960's and 1970's a great deal of work was done developing nuclear thermal rockets under the NERVA program (Nuclear Engine for Rocket Vehicle Applications) [9]. Engines tested during this time had specific-impulses in excess of 850 seconds, and showed potential for even greater performance. Because the specific-impulse of chemical rockets tops out at around 450 seconds, NTR's such as NERVA (that had solid Uranium fuel), could provide twice the Delta-v for a given inert-mass fraction. However, because the NERVA reactors used solid fuel, the maximum operating temperature was defined by the material limits of the core.

At the same time that the NERVA project was progressing in the 1960's, the AEC and NASA were also pursuing more advanced gas-core nuclear thermal rockets. With gaseous Uranium fuel, there is practically no temperature limit, and thus a gas-core engine could conceivably have a specific-impulse of thousands of seconds [10]. The open-cycle form of the engine would allow the fuel and propellant to come into direct contact, with the fuel confined by hydrodynamic forces (caused by the flowing propellant) in the center, which would heat the propellant through radiation. A number of reactor criticality tests and cold-flow tests were conducted to determine how feasible the concept was, but no rocket engine was ever tested [11], [12], [13]. Although there was a great deal of work done studying both reactivity effects and fuel leakage (including a number of cold-flow experiments) [14], [15], [16], more realistic simulations and models

weren't developed until more recently. Some of these newer studies employing modern CFD codes have found additional complications to both leakage and reactivity caused by instabilities and vehicle acceleration [2], [17], [18].

Later work at NASA in the early 1970's proposed an engine that gets around many of those issues. This is the Mini-Gas Core concept, and was already discussed extensively in the previous chapter.

The gas-core rocket is very well suited for either fast, or very efficient crewed missions to deep space. The most likely deep space destination for any crew in the foreseeable future is Mars, and so spacecraft masses (including scientific equipment and consumables for the crew) have been examined in great detail by NASA [6]. The most recent such study was done in 2009, and uses the most up to date data available for masses, but also Δv vs. launch window for missions ranging from the mid 2030's to the late 2040's. This data was used to estimate vehicle masses for the hybrid-core concept, and also for an alternative mission architecture that uses more of the available resources on Mars (to further reduce all-up launch mass) than the NASA study.

Conclusions

Although there has been a great deal of work done to study gas-core rockets over the last 50 years or so, there are still significant problems that have yet to be solved. Mainly, issues with reactivity fluctuations and fuel leakage. Some of these problems would be minimized by adding a solid-fuel driver core around the cavity, but previous concepts are severely limited in power to the point of not being competitive with other systems.

The main focus of this work was to show that a hybrid-core rocket could be made that could be cooled entirely by propellant, thus eliminating the power limitations, while retaining containment and reactivity stability benefits.

The performance of such an engine should be great enough to make multiple round trips to Mars. This eliminates the need to launch an entirely new transfer vehicle for each mission, merely the (modest) amount of propellant needed for the trip.

Chapter III: Methodology

Research Approach

The goal of this work was to show that a hybrid cavity/solid core reactor could have greater performance than a solid core NTR, smaller reactivity changes than a gas core, and higher power and thrust than the Mini-Gas Core rocket. However, the focus was more on reactor physics than thermal-hydraulics due to the extra time it would have taken to learn a CFD code, and because fuel containment has already been more widely studied. The fluid mechanics of this reactor would remain much the same as those other engines in principle. However, the result of this is that leakage cannot accurately be estimated for a given hybrid engine, but with semi-empirical relations for various leakage mechanisms leakage can be roughly compared to a pure-gas engine. Again the comparison is only indicative, but still shows the potential benefits.

Because the goal was to simply show a comparison between the hybrid rocket and the pure-gas rocket, three engines were studied that all had identical core geometry with the exception of the relative fuel quantities. This allowed all the relevant parameters to be directly compared from one engine to the next. Further, two different hybrid cores were studied with different ϵ_{gas} values to see how reactivity fluctuations and thermal hydraulics can vary depending on the engine design to highlight possible tradeoffs, and hopefully showing that reactor control would be easier.

Finally, with assumed leakage rates, the performance of each engine was determined with a NASA chemical equilibrium code [19] so that additional design tradeoffs could be examined in the context of realistic missions. This only provided a

rough estimate of I_{sp} since the code was designed to evaluate the performance of chemical rockets.

MCNP6 and Basic Reactor Physics

The majority of the work here was done in MCNP6. This allowed determination of critical masses, reactivity changes for various perturbations, and energy deposition in reactor components for realistic designs. A few simplifying assumptions were made in building the reactor models. Exterior engine components such as turbo-pumps, shielding, and thrust structures were assumed to have negligible reactivity worth, and so were left out. However, as much of the interior components as possible were included. The nozzle, cooling jacket, and pressure vessel were designed and sized as they would be for an actual engine.

Before detailed engine models were developed in MCNP, a simpler model was studied using MCNP to find the approximate critical dimensions of such a reactor, and to see if it were possible to get values of ϵ_{gas} around 50%. The simpler model evaluates more quickly, which is important since complicated MCNP models with realistic neutron source distributions can take hours to run, even on relatively fast PC's. Although the model was not as accurate as the final engine models, it be could run, modified, and re-run very rapidly. This provided a starting point for sizing and composition of the more detailed models. An illustration of this rough model is shown in Illustration 4.

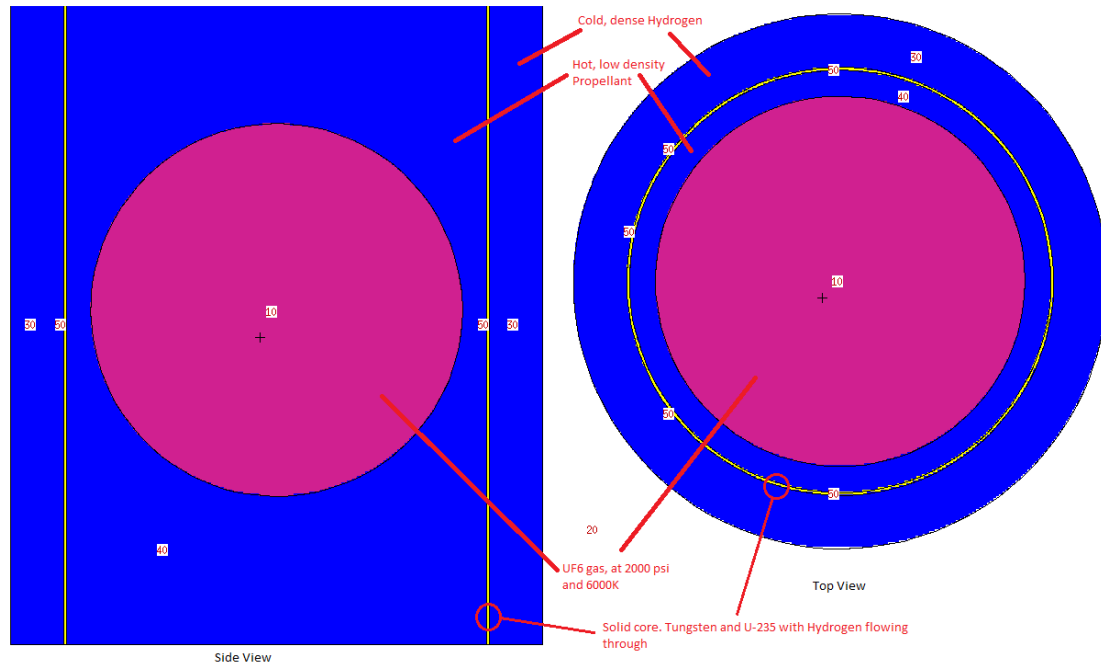


Illustration 4. Basic MCNP model (the two views are cross sections)

The density of the fuel (high enriched $^{235}\text{UF}_6$) was roughly estimated with the ideal gas law. However, at these temperatures, the ideal gas law is a poor approximation, and later models used the Van Der Waals equation to more accurately estimate the fuel density. The fuel had an assumed temperature of 6,000K and a pressure of 13.8 MPa (2000 psi), which is somewhat conservative compared to the conditions in previously studied gas core rockets [17]. This core is approximately 2m tall, and 2m in diameter. This initial core was assumed to have Tungsten foam and UO_2 in the solid core instead of graphite foam and UO_2 , but the composition of the fuel matrix makes little difference. The ϵ_{gas} was about 50% in the final iteration. Assuming the wall is made from 4140 steel with an ultimate tensile strength of 0.862 GPa (125 ksi), and the density is 7830 kg/m^3 [1], the resulting thickness for the (thin-walled) cylinder is about 2cm (using a safety factor of 1.25), and it has a mass of about 2000 kg. This simple model did not have a pressure vessel included in the MCNP model, and using composites such as carbon-fiber would

reduce the weight significantly. Therefore, the other models use graphite/epoxy pressure vessels, which are included in the MCNP models.

To determine ϵ_{gas} , the relative amounts of power deposited in the reactor components needs to be measured. MCNP sees the model as a combination of numbered cells (the cell numbers are apparent in the above illustration). There was no assumed overall reactor power, since MCNP does not find time-dependent solutions. Instead, neutrons are initiated in some distribution in one or more cells, and the energy deposited in each cell per source neutron is tallied. There are numerous types of tallies available, but the one used here is a special energy deposition tally that accounts for all sources of energy (such as fission, radiation, and kinetic energy from subatomic particles scattering within the cell). More explicitly, the output file gives the energy per neutron per gram (MeV/g) in each cell, and the calculated mass of the cells that were included in the tally. So, ϵ_{gas} can be calculated by dividing the total energy deposited (cell tally*cell mass) in the gas fuel by the energy deposited in the whole reactor.

In addition to getting the desired ϵ_{gas} , the reactor also needs to be critical for steady-state operation. Once the system is critical, perturbations to the geometry and composition can be introduced to determine their reactivity worth. MCNP has a special k-code tally specifically for determining the reactor multiplication factor k with the given neutron source(s). Both tallies can be used together, and so the reactor can be iteratively changed until a critical system is reached that has the desired properties.

Refined MCNP Models

Once the basic model was finished, a more complete rocket engine model was developed starting with the same rough dimensions. This reactor was spherical, since

previous studies have found that spherical cavities have less fuel leakage, and spherical geometry tends to have a smaller critical volume, which would reduce the engine mass. To make the model as complete as possible, the nozzle was sized as it would be any other rocket engine.

First, to calculate the approximate throat area, some initial mass flow rates must be estimated. The reactor power was defined as 3GW, and the I_{sp} was initially assumed to be 2000 Sec. This gives a total mass flow rate of about 15.6 kg/s, and a throat radius of 4.33 cm. This is a small throat area compared to a chemical rocket of the same thrust, but the mass flow rate here is significantly smaller since the specific impulse is so much higher. The nozzle expansion ratio (ratio of exit area to throat area) was chosen to be 150:1, which is typical for a rocket engine that operates in a vacuum [1].

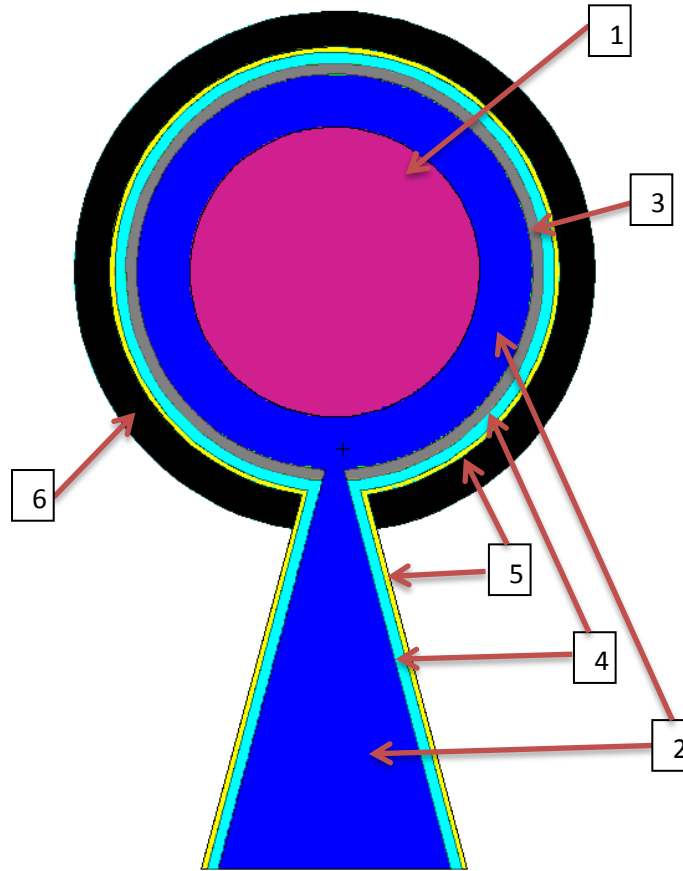


Illustration 5. Refined hybrid engine

There is assumed no material in the nozzle wall, but it is surrounded by a layer of cold propellant, and carbon-fiber outer wall (which is also part of the pressure vessel). The refined hybrid core is shown in Illustration 5. Each cell is numbered, and described in the tables below, along with the pure gas core (which has the same geometry, only without the solid fuel). The composition and assumed temperature of each cell is included. MCNP uses ENDF cross-section data for numerous isotopes including the naturally occurring mix of isotopes for each element up to temperatures of 3000K.

Table 1. MCNP model details, pure gas core

Cell Number	Description	Composition	Assumed Temperature (for ENDF cross sections), K	Nominal Dimension
1	Hot fuel plasma	UF ₆ (0.14 g/cc)	3000	Diameter = 149cm
2	Hot Propellant	H and ²³⁵ U (0.00041 g/cc, U = 1 w%, H = 99 w%)	2500	Thickness = 15.5cm
3	Solid-Fuel Core	N/A	N/A	N/A
4	Cold Hydrogen Propellant	H ₂ (0.027 g/cc)	293.6	Thickness = 5cm
5	Pressure Vessel	Graphite and epoxy (C ₂ , O and H ₃) approximate composition. 60% graphite, 40% epoxy by weight. (1.44 g/cc)	1200	Thickness = 2.4cm
6	Reflector	Graphite (2.27 g/cc)	1200	Thickness = 23.6cm

Table 2. MCNP model details, low ϵ_{gas} core

Cell Number	Description	Composition	Assumed Temperature (for ENDF cross sections), K	Nominal Dimension
1	Hot fuel plasma	UF ₆ (0.14 g/cc)	3000	Diameter = 109cm
2	Hot Propellant	H and ²³³ U (0.00041 g/cc, U = 1 w%, H = 99 w%)	2500	Thickness = 34.5cm
3	Solid-Fuel Core	Graphite (low density foam) and UO ₂ (0.75 g/cc)	2500	Thickness = 6cm
4	Cold Hydrogen Propellant	H ₂ (0.027 g/cc)	293.6	Thickness = 5cm
5	Pressure Vessel	Graphite and epoxy (C ₂ , O and H ₃) approximate composition. 60% graphite, 40% epoxy by weight. (1.44 g/cc)	1200	Thickness = 2.4cm
6	Reflector	Graphite (2.27 g/cc)	1200	Thickness = 23.6cm

Table 3. MCNP model details, high ϵ_{gas} core

Cell Number	Description	Composition	Assumed Temperature (for ENDF cross sections), K	Nominal Dimension
1	Hot fuel plasma	UF ₆ (0.14 g/cc)	3000	Diameter = 132cm
2	Hot Propellant	H and ²³³ U (0.00041 g/cc, U = 1 w%, H = 99 w%)	2500	Thickness = 24cm
3	Solid-Fuel Core	Graphite (low density foam) and UO ₂ (0.75 g/cc)	2500	Thickness = 5cm
4	Cold Hydrogen Propellant	H ₂ (0.027 g/cc)	293.6	Thickness = 5cm
5	Pressure Vessel	Graphite and epoxy (C ₂ , O and H ₃) approximate composition. 60% graphite, 40% epoxy by weight. (1.44 g/cc)	1200	Thickness = 2.4cm
6	Reflector	Graphite (2.27 g/cc)	1200	Thickness = 17.34cm

Obviously, the fuel and propellant would be much hotter than the 2500K or 3000K assumed for the material properties in MCNP. However, there is no cross section data available at the extreme temperatures the engine would actually experience, but the error introduced makes little difference for the purpose of comparing the reactors. Perhaps this is another area where further research would be needed.

One notable feature is that the cold propellant surrounds the nozzle as well as the cavity. This is because the engine is assumed to be regeneratively cooled. The cold Hydrogen would enter a manifold at the bottom of the nozzle and flow upwards into the engine. This cools the nozzle and chamber walls, while also warming the propellant. This

is quite common is liquid-propellant chemical rockets, and would be necessary here due to the high operating temperatures.

As previously discussed, the cavity and fuel size were estimated previously through trial-and-error, and further iterations were done in this model to refine the geometry until a critical configuration was obtained (the final $k_{\text{eff}} = 1.00098 \pm 0.00049$). This basic fuel geometry was modified to produce a second hybrid core with a different ϵ_{gas} , and a pure gas-core reactor. This allowed all three to be identical except in their respective solid/gas fuel quantities.

The engines also included a properly sized nozzle. For a rocket engine operating in a vacuum, there is no particular optimum nozzle size, instead it is made as large as is practical within other constraints (such as mass, launch vehicle shroud dimensions, etc.). However, for a large engine operating in space, a typical expansion ratio ($A_{\text{exit}}/A_{\text{throat}}$) is about 150:1. To estimate the throat area, the mass flow rate had to be estimated. Since the reactor power was already decided (3GW), and the I_{sp} was estimated ~ 2000 Sec., the mass flow rate could be approximated from the jet power of the exhaust:

$$\dot{m} = \frac{2 P}{(I_{\text{sp}} g_0)^2} \quad (2)$$

In this case, the total mass flow rate is about 15.6 kg/s. Because the flow is sonic at the throat, the throat area can be calculated, but the fluid properties also have to be estimated. Because this was only to determine the dimensions for a reactor physics model, rough estimates for the fluid properties of atomic hydrogen at 10,000K were used. The expression for throat area is [1]:

$$A_{\text{throat}} = \frac{\dot{m}}{p_c} \sqrt{\frac{R T}{\gamma}} \left(1 + \frac{\gamma - 1}{2} \right)^{\frac{\gamma + 1}{2(\gamma - 1)}} \quad (3)$$

Where p_c is the chamber pressure, T is the temperature, and γ is the ratio of specific heats for the propellant. The final throat area was 0.0059 m^2 , or a throat radius of 4.33 cm. This is enough information to determine the flow areas, but does not define the nozzle shape. A detailed discussion of nozzle theory is beyond the scope of this thesis, but it will be said that usually a large nozzle such as this is a parabola. However, parabolic nozzle lengths are generally described as a fraction of the length of a comparable 15° half-angle conical nozzle. Full-length parabolic nozzles are very efficient, and are the most widely used. They are also very similar in shape to the cone, and so would make no difference in reactivity, although the difference is significant in terms of nozzle efficiency. For this reason, the MCNP model uses a 15° half-angle conical nozzle, which is also easier to create using MCNP's combinatorial geometry. Also, although the other engines have slightly different mass flow rates, the throat would not change enough between them to significantly affect reactivity, so the same nozzle geometry was used for all three. The illustration below shows all three engines side-by-side. Note the lack of solid-fuel in the gas core engine, and the obvious difference in the size of the gas-fuel region.

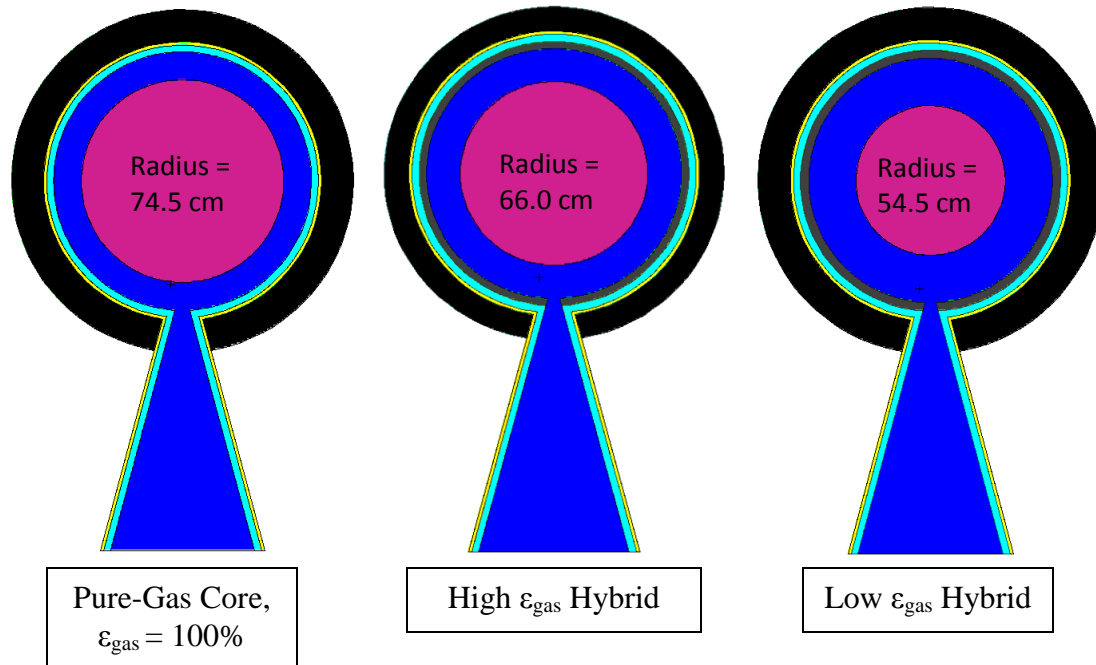


Illustration 6. All three engines (see Illustration 5, and Tables 1-3 for component labels)

Also note that the reflector for the high- ϵ_{gas} is not as thick as the other two. This was done to maximize the power ratio. It should also be noted that the two hybrid reactors had ^{233}U in the gas portion of the fuel due its higher η . This improved the ϵ_{gas} for both engines, although ^{235}U would also work, more of it would be required for a given ϵ_{gas} . However, it may be necessary since ^{233}U is not readily available at present. To show the magnitude of the effect of using ^{233}U instead of ^{235}U in the gas core, a second version of the original rough MCNP model (shown Illustration 4) was run simply replacing the fuel isotope. Since the original model was critical ($k_{\text{eff}} = 1$), and nothing else in the model was changed, the change in reactivity would be easy to determine. The effect on reactivity and energy deposition (ϵ_{gas}) are shown in the table below.

Table 4. Comparison of Energy Deposition Reactivity Change for two Gas Fuels

	²³³ U	²³⁵ U (reference)	%Δk
k_{eff}	1.13	1.00	12.74
ε_{gas}	0.64	0.57	

Because the pressure of the fuel is so high (34.47 MPa for the refined models), the Van der Waals equation was used to find the fuel density. There was no data available for the Van der Waals constants for pure Uranium gas, but there is data for UF₆ [20] which would be used at least for startup of the reactor. Precisely determining the density of the propellant wasn't as critical, since as a gas the small density has a negligible influence on reactivity. The solid fuel regions in the two hybrid reactors only differ in the thickness of the fueled region (by 1 cm). Below is a table summarizing the isotopic composition of the fueled regions in the reactors.

Table 5. Fuel composition of each core

	Composition		Density (g/cc)
Pure Gas Reactor	²³⁵ UF ₆		0.1402
	Solid fuel	C (97.728 w%), ²³⁵ U (2 w%), O (0.272 w%)	0.75 (foam)
Hybrid Reactors	Gas fuel	²³³ UF ₆	0.1402

Another result of the high pressure is a fairly substantial pressure vessel. This could very well affect reactivity, so it needed to be properly sized just like the nozzle. As mentioned previously, the vessel was assumed to be made from carbon-composite with 60% graphite by weight, and 40% epoxy. The wall thickness is easy to determine once

the yield strength and safety factor are known. A typical safety factor for spacecraft structures is 1.25 (a small margin to minimize weight), the ultimate tensile strength for an isotropic layup of carbon-fiber is $F = 0.895$ GPa (130 ksi) [1], and the radius of the pressure vessel $r_c = 1$ m. The wall thickness for a thin-walled spherical vessel is:

$$t_w = 1.25 \frac{p_c r_c}{2 F} = 2.4 \text{ cm} \quad (4)$$

The density of the carbon composite is 1550 kg/m^3 , and so the pressure vessel weighs about 470 kg. So, clearly the graphite reflector would contribute much more to the overall engine mass. Assuming typical masses for other components, the fully fueled mass of all three would likely be between 7 and 10 metric tons including turbo-machinery, shielding, and thrust structures. Radiation produced while the reactor is critical will eventually break down the epoxy, but because the engine will only be running for relatively short durations (minutes to hours), it's assumed that it will still last long enough to be useful.

Solid-Core Heat Transfer

The main heat transfer mechanism in a gas core reactor is radiation, but in the hybrid reactor, up to half of the power is produced in the solid core and needs to be removed with convection.

Because the solid-core is relatively thin, the internal surface area needs to be very large to adequately heat the propellant to the maximum allowable temperature. For this reason, two different fuel-matrix materials were examined that have enormous specific surface area: Tungsten foam and graphite foam with UO_2 particles embedded within the foam ligaments. Both of these are already widely available, and have melting points well in excess of 3000K, so the temperature limit is only defined by the melting point of UO_2 ceramic, which is about 3100K. Also, both graphite (which starts decomposing around

4000K) and Tungsten (melting point 3700K) have been used in reactors [21], and their behaviors are well understood. The focus initially was on graphite foam, since it can tolerate higher temperatures, and (as foam) has a higher thermal conductivity than Tungsten foam [7] [8].

To determine the heat transfer coefficient, past studies have developed semi-empirical relationships based on the porosity and geometry of the foam. The assumed geometry is an arrangement of unit cubes with a spherical void in each, with the diameter of the sphere larger than the side of the cube. The relevant properties (such as specific surface area and pore diameter) are generally provided by the manufacturer for a given density, but the pore diameter may need to be calculated. A detailed explanation of this is beyond the scope of this paper, but the results will be used. To calculate the Nusselt number, the Reynolds number needs to be found from the pore diameter D , and propellant dynamic viscosity μ :

$$Re = \frac{\dot{m} D}{\mu 4\pi R^2} \quad (5)$$

Where R is the mean radius of the solid core ($\sim 1\text{m}$), and \dot{m} is the mass flow rate of the propellant. The Nusselt number comes from experiments that have been done with gasses flowing through the foam:

$$Nu = \begin{cases} 0.004 Re^{1.35} Pr^{1/3} & Re < 75 \\ 1.064 Re^{0.59} Pr^{1/3} & Re > 750 \\ \frac{1.064 Re^{0.59} Pr^{1/3} + 0.004 Re^{1.35} Pr^{1/3}}{2} & 750 \geq Re \geq 75 \end{cases} \quad (6)$$

Expressions for Nusselt number have only been developed for Reynolds numbers less than 75, and greater than 750. The accepted procedure to find Nu with Re in between 75 and 750 is to linearly extrapolate. However, this will rarely be needed since the foam cell

structure very quickly raises the Reynolds number above 750. The heat transfer coefficient is then:

$$h = \frac{Nu k_{th}}{D} \quad (7)$$

Here, k_{th} is the thermal conductivity of the propellant at the assumed mean temperature of 1500K. All of these values can be found in data sheets for existing foam using the density, which was already determined in the MCNP model. The resulting h is about 217 Watt/m²/K, and given the volume of the solid core (calculated by MCNP), the internal surface area is about 9690 m². The product of these is 2.1x10⁶ Watt/K. Clearly, with the large temperature change in the propellant, the 1 to 2 GW produced in the solid core will easily be transferred to the propellant, even with the relatively thin fuel matrix. This all assumes that the propellant is being fed radially inward through the matrix; in reality it would be fed more tangentially to help confine the gaseous fuel. This would improve convective heat transfer even more.

The conclusion here is that graphite or Tungsten foam would not be necessary for heating the propellant and cooling the solid fuel, and so more conventional fuel structures (such as the simple graphite core in NERVA) could probably be used just as effectively.

The necessary heat transfer from the solid-core was also used to define the mass flow rate. Assuming the initial temperature of the Hydrogen is about 290K, and the exit temperature (inlet to cavity) is 3000K, the mass flow rate is $\dot{m} = \frac{P (1-\epsilon_{gas})}{c_p (3000K-290K)}$. For the high- ϵ_{gas} engine, the mass flow rate is 17.2 kg/s, and for the low- ϵ_{gas} engine it's 28.2 kg/s. This agrees nicely with initial estimates based on assumed performance, so further iterations were not necessary. Assuming all the power produced in the gas fuel is

transferred to the propellant, then the exhaust temperatures would be ~5500K for the low- ϵ_{gas} case, and about 9,000K for the high- ϵ_{gas} case.

Reactor Cavity Heat Transfer

After the propellant has been heated by the solid fuel, it then has to absorb the energy produced by the gas fuel. This can only be done through radiation, since mixing the fuel and propellant will result in unacceptable leakage rates. This problem has already been studied in some detail in the context of gas-core rockets, and potential solutions have already been suggested. However, the radiation heat transfer still needs to be determined to find the engines performance.

First, the opacity of the propellant needs to be increased to absorb the radiation from the fuel. This would be done by adding a ‘seed’ material to the propellant such as graphite dust. The opacity κ is defined as the absorbing surface area per kg of seed material. Past studies have found that adding 0.7% of the propellant mass flow rate as fine graphite dust would provide opacity of 5000 m²/kg [3]. In a spherical core, with a spherical fuel region, the fraction of the radiation absorbed in the propellant is [3]:

$$\frac{I(R_c)}{I_0} = 1 - e^{-\kappa \rho (R_c - R_f)} \quad (8)$$

R_c is the cavity radius, R_f is the fuel radius, ρ is the propellant density, and $I(r)$ is the radiation intensity at radius r from the center of the cavity. With the opacity provided by the graphite seed, nearly all radiation is absorbed in the propellant for all three reactors. Of course, this is referring only to non-ionizing radiation (IR and visible primarily). Gamma-rays and neutrons will only carry a relatively small amount of energy out of the core. However, although it’s small enough to ignore for the sake of heating the propellant, nuclear radiation can heat up the walls significantly. MCNP accounts for that

in the energy deposition tallies, and so the cooling requirements for the engine walls can also be estimated. The result is that we can safely assume all of the Black-Body radiation is absorbed in the propellant in all three cases.

The original assumed temperature for the Uranium plasma was 10,000K. To determine the actual equilibrium temperature, we use ϵ_{gas} to find the power generated in the gas fuel, and the surface area of the fuel using the Stefan-Boltzmann law (assuming an emissivity = 1):

$$T^4 = \frac{P \epsilon_{\text{gas}}}{(4\pi R_f^2)\sigma} \quad (9)$$

The resulting equilibrium temperature (assuming the propellant doesn't reflect any radiation back in) for all three is between 9000K and 10,000K, so the initial assumption was clearly very close.

Therefore, determining the final exhaust temperature was trivial, since the entirety of the power produced in the gas core is transferred to the propellant. Given the known mass flow rate and heat capacity, the temperature change is simply $\Delta T = \frac{P \epsilon_{\text{gas}}}{\dot{m} c_p}$. Because the initial temperature for the hybrid engines is 3000K, an increase of 2500K would result in an exhaust temperature of 5500K, which is enormous. This is likely even if ϵ_{gas} is 50%, because the specific heat capacity is greater at higher temperatures, i.e. $c_p = 18.39$ KJ/kg/K at 3000K and $c_p = 20.61$ KJ/kg/K at 5500K.

Chemical Equilibrium and Specific Impulse

Finally, to determine the specific impulse for the three engines for comparison, the precise chemical composition, and by extension, the mean molecular weight and adiabatic index had to be determined with a computer code. These codes have been developed for chemical rockets, and are readily available, but for exhaust compositions

nearing 10,000K, there is no code that is very accurate. However, after testing several different codes against known results, NASA's CEA (Chemical Equilibrium Applications computer code) appeared to be the most accurate. CEA is able to account for ionization and dissociation of species, and will continue calculations until the temperature >20,000K.

The code is fairly straightforward. All of the chemical reactants are added individually with their respective weight fractions, and initial temperatures. The software uses a comprehensive database of chemical properties to find the most common exhaust products, and compute the bulk properties such as molecular weight and ratio of specific heats. For evaluating a chemical rocket, there are three ways to evaluate the performance. One is frozen equilibrium; where the chemical properties in the combustion chamber are assumed to be the same at the throat and in the nozzle. Shifting equilibrium continues evaluating the chemical reactions at all stations in the engine. Finally, the chamber pressure and temperature can be assumed constant (and need to be defined by the user). It's this option that has to be used for a nuclear thermal rocket. In this mode, the code does not provide the exhaust velocity or vacuum I_{sp} ; instead, the resulting fluid properties must be used to calculate it.

Because the code was designed to be used for chemical rockets, the results for the extremely high-temperature gasses here may be more accurate than simply assuming what the thermodynamic properties of the exhaust would be, but not good enough to design a real engine. The calculated exhaust velocity for all three engines was slightly too high to be realistic, resulting in jet-powers of ~3.5 GW. To approximate the expected performance, the exhaust velocities were calculated using eq. (1) on page 1 with the

thermodynamic CEA results, and were averaged with the exhaust velocities from ideal estimates based on reactor power, which is more conservative.

Mission Analysis

Once the specific impulse and approximate system mass are known, possible missions can be examined. For all three engines, the power is 3GW and the thrust is on the order of 300kN, this assumption was deliberately chosen so that they could be used in a large crewed vehicle. The performance of these engines is great enough to potentially enable human missions virtually anywhere in the solar system, but the most likely use would be in a Mars-bound spacecraft. For this type of mission, spacecraft and system masses, Δv 's vs launch windows, and mission scenarios have already been thoroughly studied by NASA [6]. The NASA study also looked at NTR's for propulsion, albeit solid-core NTR's. The general spacecraft configuration is shown below.



Advanced Propulsion – Depiction of NTR propulsion Mars transfer vehicle in LEO prior to departure. Glenn Research Center 2007.

Illustration 7. NASA NTR MTV (image courtesy of NASA)

The vehicle in question is merely a transfer vehicle. It takes the crew from low earth orbit to low Mars orbit, and then back to Earth orbit again. This is the model for the vehicle used here. Using the I_{sp} 's for the three engines and the Δv 's estimated for all of the maneuvers required for a conjunction class mission (where the crew remains on Mars for a full Martian year), the propellant masses were estimated and compared to the NASA vehicles. The results suggested another type of mission architecture where the MTV Earth-return propellant (Hydrogen, Ethane or Methane) would be produced on Mars, in addition to the chemical propellant for the Mars ascent vehicle which carries the crew off of the surface of Mars and into low Mars orbit for rendezvous with the MTV. However, this is contingent on Hydrogen being produced on the surface of Mars. This should be possible since water (liquid and solid) is now known to exist over large areas of Mars [22], [23].

Chapter IV: Results

Power Ratio Determination and Cooling Requirements

As discussed previously, one of the most important parameters is the power ratio, because this used to determine the overall engine performance and heat transfer requirements for the solid core. The energy deposition tally in MCNP was also used to determine the cooling requirements for nominal hybrid reactor components. The tables below summarize the energy deposition for both of the hybrid cores. The tally results produced by MCNP are defined in terms of the energy deposited per input neutron. Each simulation has an explicit number of input neutrons (defined by the user) which get multiplied or lost, and cause other reactions and produce other particles. The energy deposited from all particles can be tallied in each cell. This can then be used to find the fraction of the reactor power that is deposited in each cell.

Table 6. High- ϵ Engine Energy Deposition

Component Name	Energy deposited (MeV/source neutron)	Percentage of whole:
Gas Core	46.94	67.30%
Hot Propellant	0.05	0.07%
Solid Core	21.65	31.04%
Pressure Vessel Wall	0.55	0.78%
Reflector	0.56	0.80%
Total:	69.75	

Table 7. Low- ϵ Engine Energy Deposition

Component Name	Energy deposited (MeV/source neutron)	Percentage of whole:
Gas Core	36.13	51.50%
Hot Propellant	0.07	0.10%
Solid Core	32.81	46.77%
Pressure Vessel Wall	0.54	0.77%
Reflector	0.61	0.86%
Total:	70.14	

To determine the total heat transfer in the solid core, the inlet temperature had to be determined from the cooling requirements for the reactor's passive components (assuming the core is regenerative cooled). The mass flow rate is determined by the cooling requirements and melting point of the solid core. Assuming the Hydrogen enters the engine at 22K, the reactor total thermal power is 3GW, then the temperature increase due to radiation and neutrons absorbed in the reflector and pressure vessel wall would heat it 200K. Therefore, the inlet temperature to the solid core is very nearly room temperature, which is very close to the initial temperature of the cold propellant jacket assumed for the MCNP simulations (although it makes little difference to the cross sections).

Critical Mass Comparison

Another interesting point of comparison between all of these reactors, and could be another advantage for the hybrid reactor over the pure-gas reactor is the overall critical mass. One might expect the hybrid core to have a reduced critical mass simply because of the higher fuel density in the solid core. Indeed, that's what was found. When the MCNP models were being designed, the solid-fuel thickness and fuel concentration were only iterated until the desired power ratios were attained, and each of the three systems was critical. MCNP automatically calculates the total mass of each cell, and this is given in the output file. Because the fuel concentration was defined as a weight fraction (relative to the graphite in the fuel matrix), the total fuel mass is trivial to calculate. The table below shows the critical masses for the three engines.

Table 8. Critical Masses

	Gas Fuel Mass [kg]	Solid Fuel Mass [kg]
Low- ϵ Engine	63.8, ^{233}U	9.56, ^{235}U
High- ϵ Engine	113.4, ^{233}U	8.06, ^{235}U
Pure-Gas Engine	163.5, ^{235}U	N/A

Clearly, there is a very sharp decrease in the amount gaseous fuel required, with only a very small increase in the amount of the solid fuel. The net effect is a tremendous reduction in the critical mass and overall fuel cost for the hybrid engines, and especially for the low- ϵ_{gas} engine. This is especially important if ^{233}U is used as the gaseous fuel, since it would have to be bred specifically for this purpose, making it very expensive.

Reactivity Effects

Because most of the fuel is amorphous, there are a large number of things that could cause its geometry to change during operation. The fuel plasma could move within the cavity due to the vehicle accelerating, swell or compress (changing the density), or leak into the propellant in various amounts. Additionally, there are other possible changes that could affect reactivity that need to be investigated such as the addition of seed material, and the loss of propellant in the cavity (such as what happens at startup and shutdown when there is little or no propellant flow).

The first of these is the density change. The density in the cavity could change wildly if there is inadvertent acoustic instability, such as is common in chemical rockets, and other studies have shown may be problematic in gas-core nuclear rockets too [17]. For finding the reactivity change, batch runs were done in MCNP, where each simulation had a different fuel density. The total fuel mass was held constant while the volume was changed (either increased or decreased which conversely decreased or increased fuel

density). The delayed neutron fraction was calculated as an average of the two different fuels (solid ^{235}U and gas ^{233}U) weighted by the relative power ratios: $\beta_{ave} = \beta_{gas}\epsilon_{gas} + \beta_{solid}\epsilon_{solid}$. Below is a plot showing the relative change in reactivity vs fuel radius. The units on the abscissa are in dollars of reactivity to help make the magnitude of the changes clear.

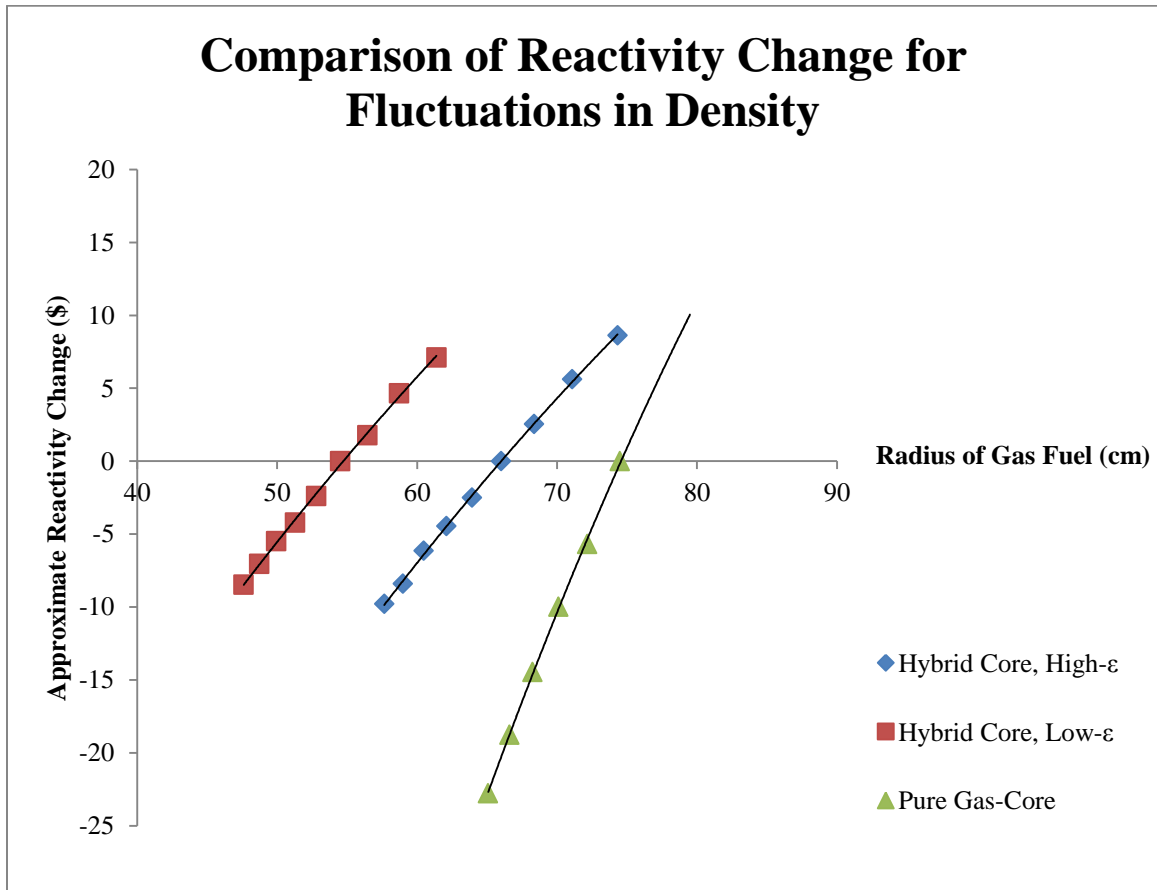


Figure 1. Fuel Radius vs Reactivity Worth (note the difference in slopes)

The swings in reactivity could be catastrophic for any of the engines if the density varies by as little as 10%. It's interesting to note that although this data is static, some inferences can be about what would happen during such a transient. As the fuel region swells and the density decreases (which corresponds to higher temperatures in the fuel, and higher power), there is a large positive reactivity change. These two things will feedback and

increase reactivity further. It's worth noting that the major cause for this large change in reactivity is the change in circular cross section of the fuel which is very opaque to neutrons. As the radius decreases, neutrons coming from the solid core or reflector are less likely to be absorbed in the fuel.

Therefore, it's worthwhile to extrapolate the data to find the extreme limits of what could be tolerated by the control system in actual operation. The density change (and also pressure) corresponding to \$1 of positive reactivity was found for all three engines, which defines the cutoff between prompt-critical and delayed-critical. Once the reactor becomes prompt super-critical, there is no hope to control it since the reactor period will be too short. Below is a table that shows how the maximum allowable swing in density and pressure (assuming the reactors start at 5000psi).

Table 9. Maximum Allowable Density Change Corresponding to \$1 worth

	Density Change [ρ/ρ_0]	Pressure Change [psi]:
Low- ϵ Engine	0.9408	295.89
High- ϵ Engine	0.9627	186.46
Pure-Gas Engine	0.9813	93.25

These are fairly large changes in pressure, but if there is undamped acoustic instability, the pressure could possibly reach these values. However, the hybrid reactors require much higher pressure fluctuations to reach prompt criticality, and so would be easier to control if instability arose.

Four other possible effects were also examined; fuel displacement aft due to acceleration, loss of propellant in cavity, the addition of seed material (graphite), and leakage of fuel into propellant (and so there is fuel mixed homogenously with the propellant). The displacement of the fuel was the same for all three engines, 15cm. The

exact displacement due to a particular acceleration would depend heavily on the vehicle design, and it changes over the course of a burn. Also, since it was merely for comparison purposes, the displacement could be chosen arbitrarily. An illustration of this from the MCNP plotter is shown below.

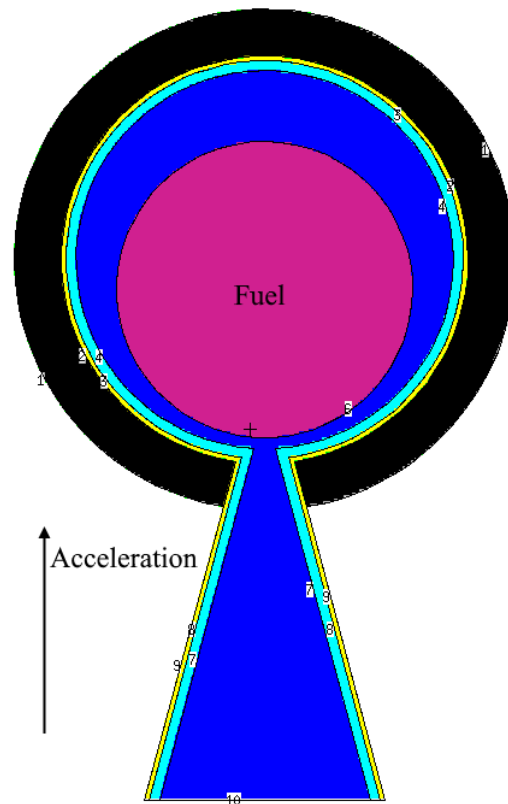


Illustration 8. Fuel Displacement Due to Acceleration

The graph below summarizes the reactivity worth of three of these perturbations. The possible reactivity effect of fuel leaking into the propellant was also examined. It was modeled in MCNP by adding fuel to the propellant as a fraction of the total propellant mass. The worth of fuel leakage into the propellant was found to be very small, $<0.1\%$ Δk for all engines and leakage rates up to 5% of the total mass flow rate. Therefore, it is

apparently an insignificant factor. If the leakage rate is greater than 5% of the mass flow rate, the engine performance will be lower, and fuel costs will unacceptably high.

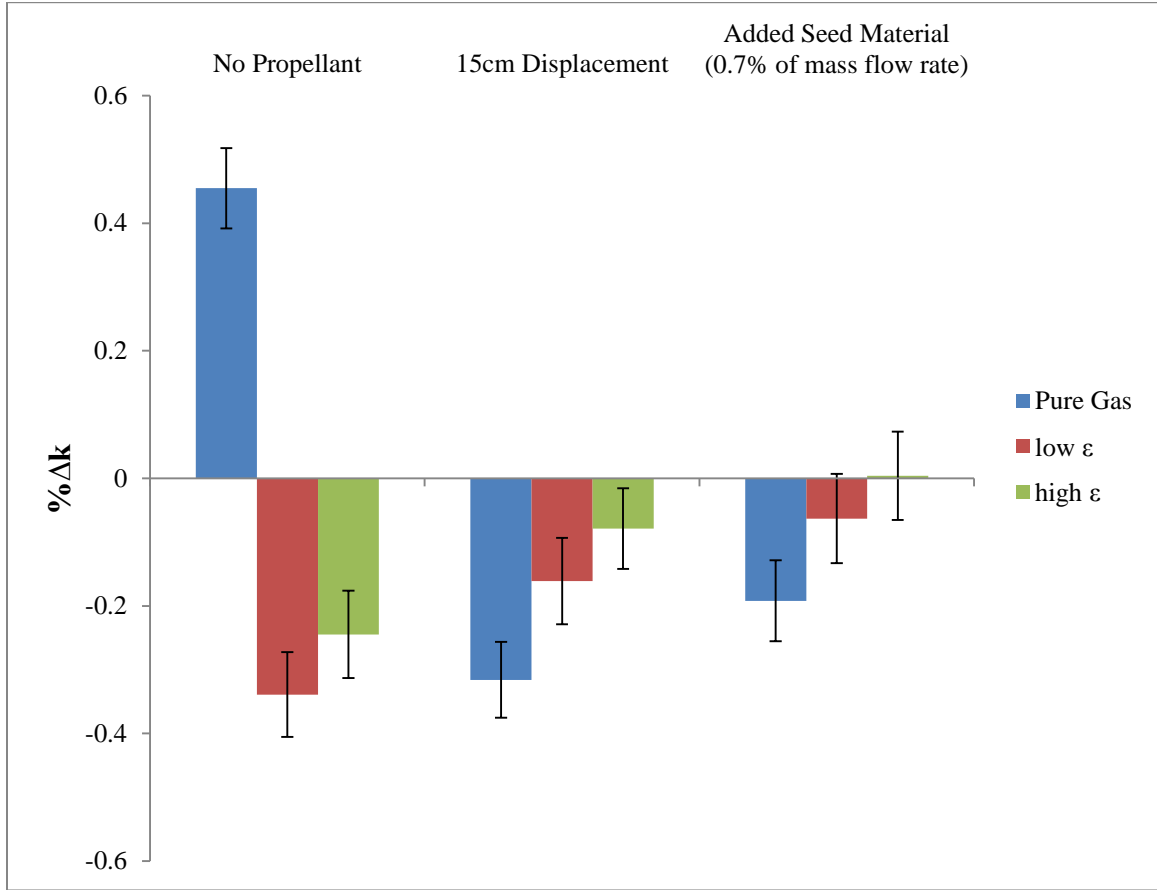


Figure 2. Reactivity Worth of Various Perturbations

The error bars on the figure are based on the standard deviation of the k 's produced by the MCNP k-code. Because the reactivity worth ($\% \Delta k$) had to be calculated, the error bars are the result of error propagation. In general, the standard deviation in a calculated result is:

$$\sigma_f = \sqrt{\left(\frac{\partial f}{\partial x}\right)^2 \sigma_x^2 + \left(\frac{\partial f}{\partial y}\right)^2 \sigma_y^2 + \dots} \quad (10)$$

Where f is a function of the measured quantities (x, y, \dots), and σ is the standard deviation of quantity of interest (f, x, y, \dots). In this case, $f = 100 \frac{k_1 - k_0}{k_0}$ (since we are calculating a percentage), so that σ_f is:

$$\sigma_f = \sqrt{\left(\frac{\partial}{\partial k_1} \left\{100 \frac{k_1 - k_0}{k_0}\right\}\right)^2 \sigma_{k_1}^2 + \left(\frac{\partial}{\partial k_0} \left\{100 \frac{k_1 - k_0}{k_0}\right\}\right)^2 \sigma_{k_0}^2} \quad (11)$$

Where k_i is the multiplication for the perturbed case, and k is nominally equal to 1 since the reference case is critical. For all cases σ_f is about 0.06 % Δk , and $k_0 \approx 1$.

Not surprisingly, the worth of the perturbations in the hybrid reactors is once again smaller in proportion to the amount of solid fuel present. This reactivity “dampening” from the solid core appears to be a great advantage of the hybrid rocket. What’s interesting though, is the effect of a void in the cavity (in place of propellant). For the hybrid reactors this is a negative reactivity, most likely because the Hydrogen propellant is acting like a moderator in between the two fueled regions. If the propellant acts more like a poison in the pure gas core, greater negative reactivity would have to be added to shut the core down after a burn and the propellant flow has been shutoff.

Fuel Leakage

Another important phenomenon unique to open-cycle gas cores is fuel leakage. This is a complex subject, and nearly impossible to adequately address without experiments or CFD simulations. However, it can be at least partially addressed (for the purpose of comparing the three engines) using empirical models that have already been developed. Past studies have identified a number of mechanisms that could cause the fuel to leak out with the propellant [17]. There aren’t empirical models for all of these, so the

goal here is to simply approximately compare the pure-gas rocket to the hybrid rockets to illustrate any significant difference in leakage.

There are three separate leakage mechanisms used here to compare the engines. Two of these are instabilities, and the third is simply normal leakage. For all of these, there are semi-empirical formulas for reactors with similar size, shape, and power level to the ones being studied here [16], [17]. The basic approach was to use these correlations to find an approximate fuel mass flow rate, and then find the leakage rate as a ratio of that fuel mass flow to the propellant mass flow rate. The leakage rates for the hybrid cores were then compared to the pure-gas core leakage rate by another ratio. The actual leakage rates were quite high, and probably not realistic, but when compared directly to a pure gas core, at least order-of-magnitude comparisons can be made.

The first mechanism is Kelvin-Helmholtz instability. The mass flow rate of fuel out of the core can be approximated as [17]:

$$\dot{m} = 4\pi R^2 F \quad (12)$$

Where R is the inside radius of the core, and F is the particle flux, defined as mass per unit area per unit time ($\text{kg}/\text{m}^2/\text{s}$) of fuel from the core of radius R . The particle flux is a function of the diffusion coefficient for fuel mixing into the propellant D (m^2/s), and fuel radius (for a spherical fuel region), R_{fuel} [17]:

$$F = \frac{D \rho_{fuel}}{R_{fuel}} \quad (13)$$

The diffusion coefficient is a function of the wave number for the oscillation k (m^{-1}), and the instability growth rate γ (s^{-1}) [17]:

$$D = \gamma/k^2 \quad (14)$$

The wave number and instability growth rate for Kelvin-Helmholtz instability respectively are expressed as [17]:

$$k = \frac{g \rho_{fuel}}{v_{prop}^2 \rho_{prop}} \quad (15)$$

$$\gamma = v_{prop} k \sqrt{\frac{\rho_{prop}}{\rho_{fuel}}} \quad (16)$$

Where v_{prop} is the velocity of the propellant moving through the cavity, which was simply assumed to be 5 m/s (a typical value) for all the reactors, and the ρ 's are the densities of the two fluids. The reason that the wave number and growth rate are separated instead of being combined is that this same treatment is used for acoustic instability, but with different expressions for k and γ .

For acoustic instability, the critical wave number and instability growth rate are expressed as [17]:

$$k_c = \sqrt{\frac{3}{2} \frac{P_{fuel}}{T_0 K_R}} \quad (17)$$

$$\gamma = \frac{K_R}{15 k_{boltz} N} (k_c^2 - k^2) \quad (18)$$

Here K_R is the singly ionized radiation diffusion coefficient (the fuel plasma is assumed to be singly ionized), N is the fuel number density, P_{fuel} is the power density in the fuel plasma (watt/m³), T_0 is the fuel temperature, k_{boltz} is Boltzmann's constant, and k is the wave number for acoustic instability $k = 2\pi/R_{fuel}$. The critical wave number corresponds to an oscillation wavelength equal to the cavity radius. The radiation diffusion coefficient is expressed as [17]:

$$K_R = \frac{16}{3} \frac{\sigma_B T_0^3}{\kappa_R} \quad (19)$$

σ_B is the Stefan-Boltzmann constant and κ_R is the mean opacity of the propellant (the same opacity used for heat transfer calculations, see Eq. (8)). This yields the leakages

relative to the pure-gas core: $r = \left(\frac{\dot{m}_{fuel}}{\dot{m}_{prop}}\right)_{gas-core} / \left(\frac{\dot{m}_{fuel}}{\dot{m}_{prop}}\right)_{hybrid}$. Since the propellant

flow velocity was chosen arbitrarily, it would be interesting to see how these ratios vary over a range of flow velocities. The flow velocity is another variable that may affect the design a real engine. It's interesting to note that the difference in leakage is not simply proportional to the difference in the amount of fuel. The plots in the figures below illustrate this.

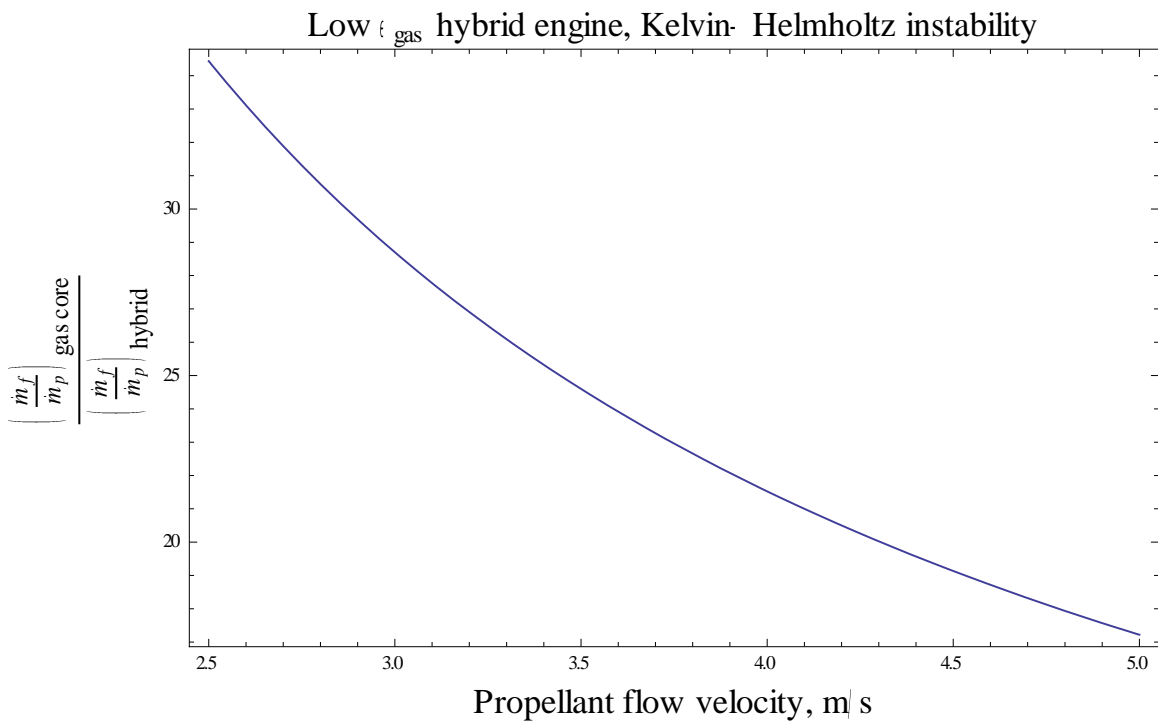


Figure 3. Low- ϵ Engine Relative Leakage due to Kelvin-Helmholtz Instability vs Flow Velocity

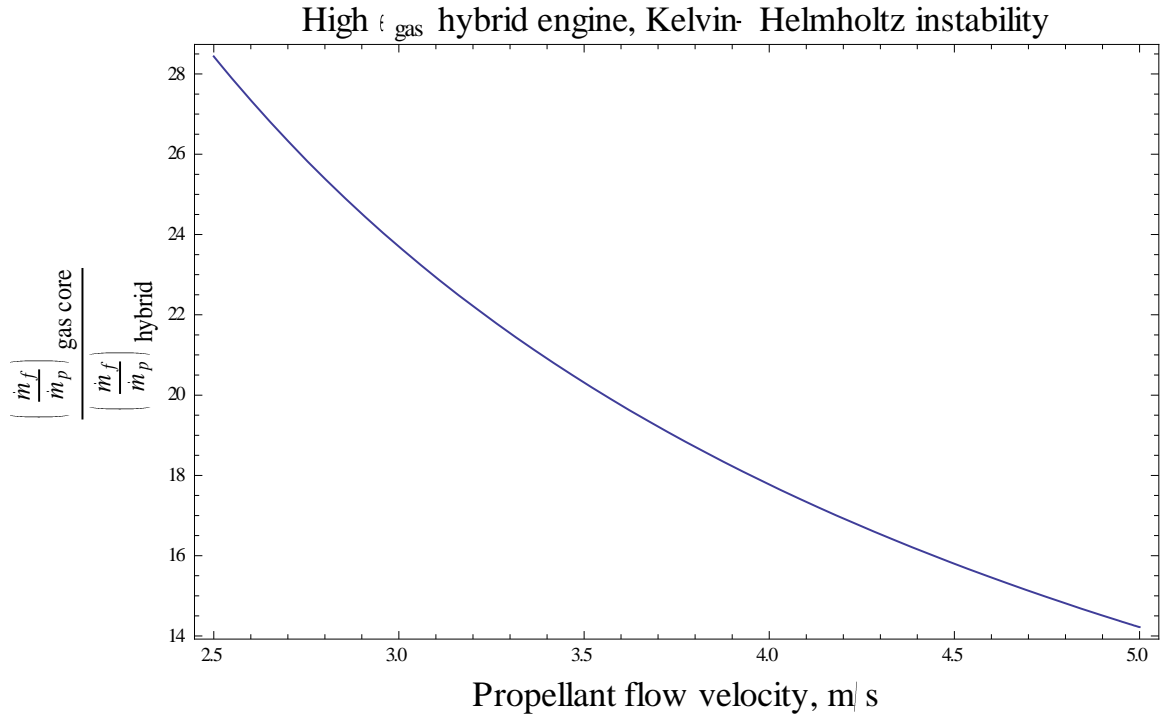


Figure 4. High- ϵ Engine Relative Leakage due to Kelvin-Helmholtz Instability vs Flow Velocity

Clearly, although these are only crude estimates, the potential of a hybrid core over a pure-gas core could be significant, at least for flow instabilities. The leakage during normal operation was also compared for the sake of completeness.

For the instability models borrowed from [17], the cavity and fuel were always assumed to be spherical. However, the only leakage model available based on experimental data and simulations were for a core with a cylindrical fuel region with an aspect ratio of 2:1 [16]. However, the reactor in question was still very similar in size to again allow for an order-of-magnitude leakage comparison between the gas-core and the hybrid cores. The relationship is related to the void fraction in the cavity, the radii of the cavity and fuel, and the densities of the fuel and propellant:

$$\frac{\text{fuel volume}}{\text{total volume}} = 1.95 \left(\frac{\dot{m}_{prop}}{\dot{m}_{fuel}} \right)^{-1/2} \left(\frac{\rho_{fuel}}{\rho_{prop}} \right)^{-3/8} \left(\frac{R_{fuel}}{R_{cavity}} \right) \quad (20)$$

Since the geometry of the three reactors is known, this can simply be solved for the ratio of the mass flow rates. This relationship also suggests that the leakage can be minimized by changing the core geometry, but for the sake of comparison, all three reactors were still assumed to have identical geometry. The results of all these scenarios are summarized in the table below.

Table 10. Relative Leakage, r for all Scenarios

	Kelvin Helmholtz Instability	Acoustic Instability	Normal Operation
Low- ϵ Engine	17.22	3.0	2.71
High- ϵ Engine	14.22	2.21	1.15

Although these estimates are only meant to be a crude indication, they all seem to indicate that the hybrid cores would indeed have reduced fuel leakage. This is an area where more research still needs to be done.

Specific Impulse and Mission Architecture

The final parameter to consider is specific impulse. As previously discussed, this was largely determined using the properties of the propellant provided by NASA’s CEA code. Because the code tended to produce results that were far too optimistic. So, the CEA results were averaged with the I_{sp} calculated from reactor power and the estimated mass flow rates (see Eq. (2)). The final results are perhaps still a bit optimistic, but are closer to reality than the CEA output alone. This is another area where better modeling tools may be needed for more advanced studies.

The overall performance results are shown in the tables below, along with the CEA input assumptions such as propellant temperature and Uranium concentration (in

weight percent). Each model included 0.7% by weight graphite seed in the input, in addition to the Hydrogen and Uranium. Since the precise leakage could not be reliably calculated, the performances for a range of leakages are included.

Table 11. Low- ϵ Engine Performance Results

Propellant Temp (K): 5740 I_{sp} (Sec.) from power: 1487.2					
Leakage (% of mass flow rate)	M (g/mol)	γ	V_e (m/s)	I_{sp} (Sec.)	Mean I_{sp} (Sec.)
0	1.519	1.3631	15358.46	1565.59	1526.37
1	1.534	1.2376	18002.39	1835.11	1661.13
2	1.55	1.2376	17909.24	1825.61	1656.38
3	1.566	1.2376	17817.51	1816.26	1651.71
4	1.582	1.2376	17727.18	1807.05	1647.10
5	1.599	1.2376	17632.69	1797.42	1642.29
10	1.688	1.2376	17161.56	1749.39	1618.28

Table 12. High- ϵ Engine Performance Results

Propellant Temp (K) 9000 I_{sp} (Sec.) from power 1899.5					
Leakage (% of mass flow rate)	M (g/mol)	γ	V_e (m/s)	I_{sp} (Sec.)	Mean I_{sp} (Sec.)
0	1.067	1.6166	19176.02	1954.74	1927.11
1	1.077	1.4827	20659.58	2105.97	2002.73
2	1.088	1.4827	20554.87	2095.30	1997.39
3	1.099	1.4827	20451.75	2084.79	1992.13
4	1.111	1.4827	20341.00	2073.50	1986.49
5	1.127	1.4827	20196.09	2058.72	1979.10
10	1.186	1.4827	19687.33	2006.86	1953.17

Table 13. Pure-Gas Engine Performance Results

Propellant Temp (K) 9000 I_{sp} (Sec.) from power 1887.5					
Leakage (% of mass flow rate)	M (g/mol)	γ	V_e (m/s)	I_{sp} (Sec.)	Mean I_{sp} (Sec.)
0	1.067	1.6166	19176.02	1954.74	1921.12
1	1.078	1.4827	20649.99	2104.99	1996.25
2	1.089	1.4827	20545.43	2094.34	1990.92
3	1.1	1.4827	20442.45	2083.84	1985.67
4	1.111	1.4827	20341.00	2073.50	1980.50
5	1.123	1.4827	20232.03	2062.39	1974.95
10	1.186	1.4827	19687.33	2006.86	1947.18

Once the specific impulse is known, the inert mass fraction can be estimated for a given orbital maneuver. An engine with such high power and efficiency like this could potentially be used for any number of advanced space missions to virtually any location in the solar system. However, a human Mars mission is perhaps the most likely, and so that is the type of mission examined here. This type of mission has also been thoroughly studied with other propulsion systems.

The specific mission examined here is referred to as a Conjunction-Class mission [6]. In this scenario, the spacecraft uses a minimum energy Hohmann transfer orbit to reach Mars, and the crew spends approximately $\frac{3}{4}$ of a Martian year on the surface before using another Hohmann transfer to return to Earth. The main alternative to this is an Opposition-Class mission. In this case, the transit time is shorter, and the crew only spends 30 to 90 days on the surface before returning. This scenario requires roughly the same Δv , and it's less appealing due to the shorter mission duration. Below are two

illustrations of the trajectories for the two types of missions, and the Δv vs launch window for each maneuver.

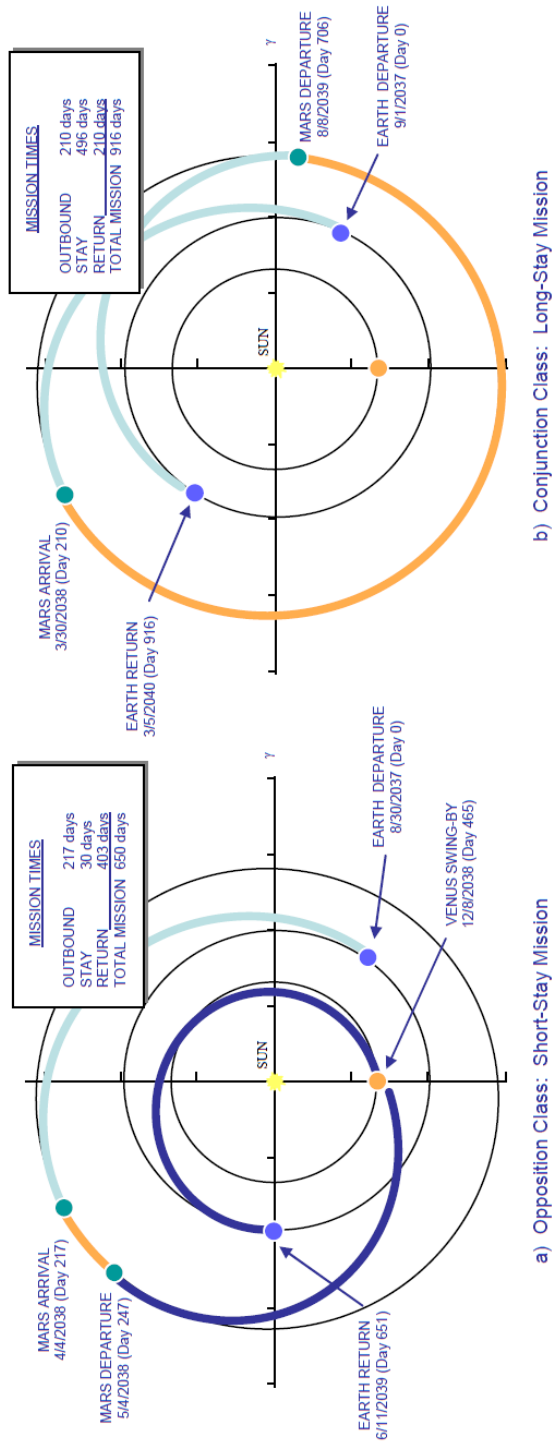


Figure 6-2. Comparison of (a) Opposition-class and (b) Conjunction-class mission profiles.

Illustration 9. Conjunction and Opposition Class Mission Trajectories (Image courtesy of NASA, [6])

All-Propulsive Crew Mission

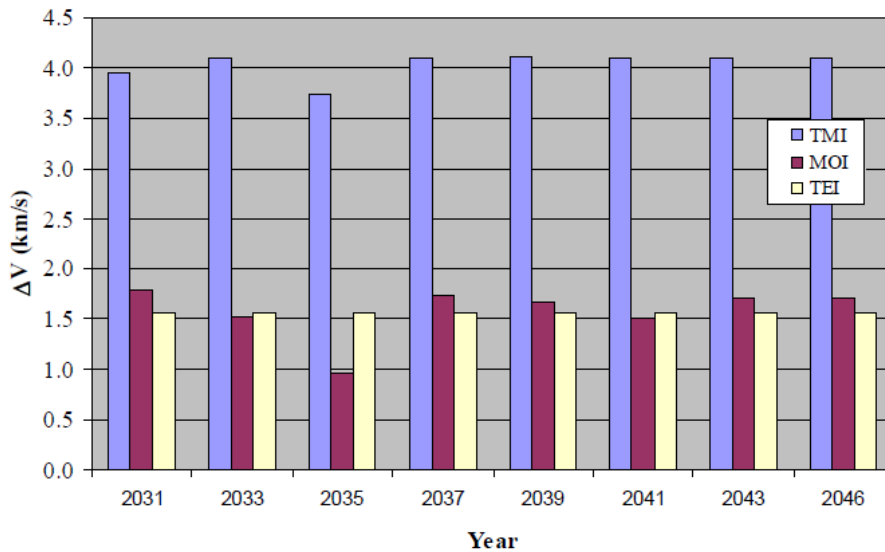


Illustration 10. Conjunction Class Δv vs Launch Window (Image courtesy of NASA, [6])

There are three main maneuvers that have to happen during a conjunction-class mission. The first is the Trans-Mars Injection (TMI) that takes the Mars Transfer Vehicle (MTV) from a low-Earth orbit to a Mars intersecting orbit around the sun. This requires a Δv of about 4 km/s. The second is Mars Orbit Insertion (MOI), which requires about 1.6 km/s slows the spacecraft and places it into Mars orbit. Finally, the Trans-Earth Injection (TEI) sends the spacecraft home, and requires about 1.5 km/s. Optionally, the transfer vehicle may make an additional maneuver to slow down upon return to enter Earth orbit so that it can be used again for another mission. This final maneuver is very difficult to do with chemical propellants due to the extra Δv . For simplicity, and to better compare with the missions outlined in the NASA architecture, the final Earth orbit injection wasn't considered. This would prevent the MTV from being reused for another mission, as it would burn up in the Earth's atmosphere upon return (after separating from the crew

reentry vehicle). Also, the Δv for the Mars Ascent Vehicle (MAV) wasn't included because its propellant is generated from resources on Mars, and is deployed ahead of the crew on a separate unmanned pre-supply mission. Below is a table of the inert mass fractions for all of these maneuvers for the hybrid rockets, the all-gas rocket, a solid-core NTR, and a typical chemical rocket. The orbits for all of these options are the same. However, the higher I_{sp} engines could be used to reduce transit times with high-speed transfers.

Table 14. Inert Mass Fractions for Mars Mission Orbital Maneuvers

	TMI	MOI	TEI
Low- ϵ Engine ($I_{sp} = 1600$ s.)	0.775	0.903	0.909
High- ϵ Engine ($I_{sp} = 1950$ s.)	0.811	0.920	0.925
Gas-Core ($I_{sp} = 1900$ s.)	0.807	0.918	0.923
NTR ($I_{sp} = 900$ s.)	0.636	0.834	0.844
Chemical ($I_{sp} = 400$ s.)	0.361	0.665	0.682

Using these inert mass fractions, and estimating the component masses based on the NASA architecture, the propellant masses for each maneuver can be estimated. Below is a table representing the propellant masses (not including lost fuel), and initial MTV dry masses. Propellant for TEI is not included here, because this would be loaded in Mars orbit. This is a comparison of the mass required to must be launched from Earth (not including pre-supply cargo).

Table 15. Spacecraft Masses and Initial Propellant Load (all units in metric tons)

	Engine, Tanks, Structure	Crew and Payload	TMI and MOI Propellant
Low- ϵ Engine	36	62.8	42.37
High- ϵ Engine	36	62.8	33.62
Gas-Core	36	62.8	34.55
NTR	91	62.8	136.1
Chemical	67.8	51.9	375.7

It's interesting to note that the pure gas core performs slightly worse than the high- ϵ engine. This is because although a pure gas core could theoretically perform much better at higher power, in this case it operates at nearly the same temperature, and the presumably higher leakage would result in a higher molecular weight exhaust and lower exhaust velocity.

The propellant requirements for the gas-core engines are of course much better, but the propellant required for TEI is small enough that the return propellant could be made on Mars and delivered to the MTV (shown in Illustration 7) with the MAV when the crew returns. The MAV (which is sent to Mars without a crew before the MTV departs) is only for returning the crew to the MTV waiting in Mars orbit, and is then jettisoned. Because the MAV will already have equipment for making Methane and Oxygen from the Martian environment, it could simply carry an empty tank that would "plug-in" to the MTV in orbit. The NASA design for the MTV already includes a saddle-truss for the propellant tank (this can be seen behind the crew module in Illustration 7), so that the tank can be jettisoned. A replacement tank could put in its place for the TEI burn. The propellant in this case would likely be Methane, which would serve as a densified form of Hydrogen. This means that the Hydrogen used to make the Methane would have to come from Mars. Past ISRU plans required the Hydrogen to be sent from Earth with the MAV. If this were necessary, then there would be no economic benefit to making MTV propellant on Mars, but if there is sufficient water/ice at the landing site, then the all-up mass of the initial pre-supply launch would be reduced, thus reducing the mission cost. This alternate scenario is shown below:

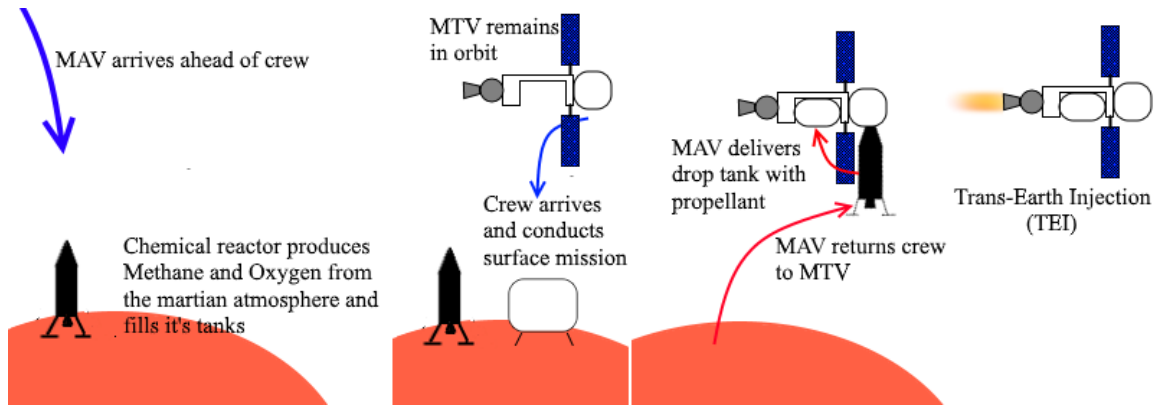


Illustration 11. In-Situ MTV Propellant Production

Chapter V: Conclusions

Discussion of Research Findings

The hybrid gas-core rocket clearly has a number of advantages over previous open-cycle engine concepts. Like the mini-gas core, the hybrid reactor could be made to be more compact due to the smaller minimum critical mass, but doesn't necessarily require external cooling. Another major advantage of the mini-gas core that this concept shares is that fluctuations in fuel geometry and composition have much smaller reactivity worth than a pure-gas core. However, the reactivity dampening is due mainly to the solid core, and so the mini-gas core would be more stable in this regard.

The reduction of gas fuel in the cavity also reduces the amount of fuel leakage, and it appears from the results for the two hybrid cores that it improves as the amount is reduced. However, if too much fuel is leaked from the cavity, the performance quickly becomes uncompetitive with advanced solid-core NTR's, indeed the assumed 1600 S. for the low- ϵ engine is quite optimistic, in reality it could be as low as 1400 S. This is another area where the mini-gas core has an advantage. The leakage may still be an issue, even for the mini-gas core, due to other mechanisms that have been studied. For instance, in [2] vehicle acceleration created by buoyancy effects was found to cause enormous leakage for accelerations as low as 0.001g. Nevertheless, a hybrid core would likely be a part of any meaningful solution.

Despite its advantages, the mini-gas core concept proposed by Robert Hyland [4] (where the core is driven mostly by a solid fuel driver) has a fatal flaw that makes it extremely unappealing relative to NTR's and electric propulsion, and that is the low operating power required to prevent the solid fuel from overheating. So, the hybrid core

is able to balance the tradeoffs between specific impulse and thrust (1500-2000 Sec., and 300kN), without sacrificing reactor control or fuel.

The specific impulse of the hybrid core is not necessary as high as the pure-gas engine (which could be as high as 8000 S.) due to the limits on the temperature, but it's significantly higher than an ordinary NTR, and produces orders of magnitude more thrust for a comparable weight than a nuclear-electric thruster could. This puts the system into a very useful niche for missions with spacecraft that require short times or heavy payloads to distant locations in the solar system.

Future Research Possibilities

As previously mentioned, one of the biggest potential issues is still fuel leakage, just as it remains for any open-cycle engine. There have been suggestions for possible solutions such as adding high-strength magnets to add pressure to the fuel to prevent mixing, and turning the whole engine upside down and turning the exhaust 180° out of the top of the reactor so that acceleration would help containment rather than hinder it. These all have issues, but haven't been thoroughly studied yet. These could benefit from multiphysics modeling and experimentation to show that they could work, and address any further difficulties.

In general, there seemed to be a lack of adequate modeling tools available. CFD would improve studies of fuel containment, but experimentation may need to be done or new computer codes need to be written to more accurately model chemical equilibrium in the engine, and better estimate I_{sp} .

Another problem that is common to all nuclear rockets, but is especially acute for an open-cycle engine is testing without releasing fission products. Current regulations

would require even a solid core NTR to fire in a closed test-cell with the exhaust fed through large scrubbers. This would be a very expensive proposition, especially since an open-cycle engine that would certainly contaminate the test cell. A practical and economical means of testing the engine would have to be found.

References

- [1] R. W. Humble, G. N. Henry and W. J. Larson, *Space Propulsion Analysis and Design*, New York: McGraw Hill, 1995.
- [2] D. I. Poston and T. Kammash, "A Computational Model for an Open-Cycle Gas Core Nuclear Rocket," *Nuclear Science and Engineering*, no. 122, pp. 32-54, 1996.
- [3] D. I. Poston and T. Kammash, "Heat Transfer Model for an Open-Cycle Gas Core Nuclear Rocket," in *Proc. Ninth Symposium on Space Nuclear Power Systems*, New York, 1992.
- [4] R. E. Hyland, "Mini Gas-Core Propulsion Concept," in *Winter Meeting of the American Nuclear Society*, Miami, Florida, 1971.
- [5] D. Buden, *Space Nuclear Fission Electric Power Systems*, Lakewood, Colorado: Polaris Books, 2011.
- [6] National Aeronautics and Space Administration, "Human Exploration of Mars Design Reference Architecture 5.0," 2009.
- [7] Q. Yu, B. E. Thompson and A. G. Straatman, "A Unit Cube-Based Model for Heat Transfer and Fluid Flow in Porous Carbon Foam," *Transactions of the ASME*, vol. 128, pp. 352-360, April 2006.
- [8] A. G. Straatman, N. C. Gallego, Q. Yu, L. Betchen and B. E. Thompson, "Forced Convection Heat Transfer and Hydraulic Losses in Graphitic Foam," *Journal of Heat Transfer*, vol. 129, pp. 1237-1245, 2007.
- [9] D. Buden, *Nuclear Thermal Propulsion Systems*, Lakewood, Colorado: Polaris Books, 2011.
- [10] R. G. Ragsdale and E. A. Willis, "Gas-Core Rocket Reactors - A New Look," in *Seventh Propulsion Joint Specialist Conference*, Salt Lake City, Utah, 1971.
- [11] J. F. Kunze, G. D. Pincock and R. E. Hyland, "Cavity Reactor Critical Experiments," *Nuclear Applications*, vol. 6, pp. 104-115, February 1969.
- [12] J. H. Lofthouse and J. F. Kunze, "Spherical Gas Core Reactor Critical Experiment," National Aeronautics and Space Administration, Idaho Falls, 1971.
- [13] R. G. Ragsdale, "Status of Open-Cycle Gas-Core Reactor Project Through 1970," National Aeronautics and Space Administration, Washington, D.C., 1971.
- [14] B. V. Johnson, "Experimental and Analytical Study of One- and Two-Component Flows in Spherical Chambers," National Aeronautics and Space Administration, 1973.

- [15] J. F. Kunze and J. H. Lofthouse, "Flow and Criticality in the Open Cycle Gas Core," in *Joint Conference on Sensing of Environmental Pollutants*, Palo Alto, CA, 1971.
- [16] H. A. Putre, "Estimates of Fuel Containment in a Coaxial Flow Gas-Core Nuclear Rocket," *Nuclear Technology*, vol. 12, pp. 209-217, October 1971.
- [17] T. Kammash and D. Galbraith, "Some Physics Issues Facing the Open-Cycle Gas Core Nuclear Rocket," in *AIAA/NASA/OAI Conference on Advanced SEI Technologies*, Cleveland, OH, 1991.
- [18] D. I. Poston and T. Kammash, "Hydrodynamic Fuel Containment in an Open-Cycle Gas-Core Nuclear Rocket," in *Proceedings of the 11th Symposium on Space Nuclear Power Systems*, Albuquerque, NM, 1994.
- [19] S. Gordon and B. J. McBride, "Computer Program for Calculation of Complex Chemical Equilibrium Compositions and Applications," National Aeronautics and Space Administration, 1994.
- [20] D. R. Lide, *CRC Handbook of Chemistry and Physics*, 85th Edition, CRC Press, 2004.
- [21] J. Lamarsh and A. Baratta, *Introduction to Nuclear Engineering*, Third Edition, Upper Saddle River, New Jersey: Prentice Hall, 2001.
- [22] e. a. F. Javier Martín-Torres, "Transient liquid water and water activity at Gale Crater on Mars," *Nature Geoscience*, 2015.
- [23] e. a. W. C. Feldman, "Global distribution of near-surface hydrogen on Mars," *JOURNAL OF GEOPHYSICAL RESEARCH*, vol. 109, 2004.
- [24] M. J. Chase, "NIST-JANAF Thermochemical Tables, Fourth Edition," *J. Phys. Chem. Ref. Data, Monograph 9*, pp. 1-1951, 1998.